NASA Technical Paper 2603

May 1986

Effects of Variables Upon Pyrotechnically Induced Shock Response Spectra

James Lee Smith

NASA

NASA Technical Paper 2603

1986

Effects of Variables Upon Pyrotechnically Induced Shock Response Spectra

James Lee Smith

George C. Marshall Space Flight Center
Marshall Space Flight Center, Alabama

NASA

National Aeronautics
and Space Administration

Scientific and Technical Information Branch

TABLE OF CONTENTS

LIST OF ILLUSTRATIONS

LIST OF ILLUSTRATIONS (Continued)

LIST OF ILLUSTRATIONS (Concluded)

TECHNICAL PAPER

EFFECTS OF VARIABLES UPON PYROTECHNICALLY INDUCED SHOCK RESPONSE SPECTRA

I. INTRODUCTION

In the 1800's, C. E. Munroe discovered that the reinforcement of shock waves in a hollow charge would concentrate the effect of the explosion along the axis of the charge; this resulting effect, the "Munroe Effect", prompted the invention of linear-shaped charges (LSCs). At that time, LSCs were used primarily in mining operations. With the advent of the Space Age in the 1950s, LSCs were used to separate boosters, cut cables, etc., on spacecraft. These precision usages of LSCs caused quality control groups to impose standards upon LSC manufacturing. Later, NASA and other LSC users developed manufacturing and assembly tolerances for LSCs and separation assemblies. No one to this date has published research findings on how these manufacturing and assembly tolerances affect shock response spectra. Evidently, no one has investigated these.

In the early 1930s, M. S. Biot devised the idea of a shock response spectra (SRS) [1]. Since that time, the majority of shock researchers and testers have measured shock in 10,000 Hz SRS. A very few companies and NASA have used 15,000 or 20,000 Hz shock response spectra. No one has investigated the higher frequency region above 20,000 Hz, primarily because sufficient instrumentation was not available. Most experts in the field did not believe sufficient energy existed beyond 20,000 Hz to cause damage to structures or components; this has been proven otherwise by this study.

One of the most comprehensive and earliest research projects in pyrotechnic shock was performed by Martin Marietta Corporation for NASA from June 1968 through March 1970. The results were reported by Kacena, Mcgrath, and Rader [2] who authored six volumes, with a seventh volume by Englesferd and Rader [3]. This study laid the groundwork for all future pyrotechnic design and research. During this study, all available pyroshock data from the industry were compiled; characteristics of pyrotechnic shock transients were defined; all compiled pyroshock data were evaluated as to "quality;" systems for measuring ground tests and flight were formulated for various structures; test simulation techniques were recommended; pyrotechnic systems were classified as to the nature of resulting shock and/or damage effects; shock characteristics as a function of structural configuration and materials were evaluated; follow-up research was formulated and recommended; shock propagation theory was applied to one class of pyrotechnic systems; and the results were compared with actual measured data; and finally, a full-scale ground test of the Titan III structure was performed to provide a basic understanding of pyrotechnic shock transient phenomena. The Martin Marietta study and the seven-volume report will be discussed in further detail in Section II.

Throughout the aerospace industry, large variations of 50 percent (6 dB) or more in SRS continue to be reported from actual flight data and from plate tests. Designers continue to overdesign to allow for these large variations.

One example of a failure due to large variations occurred during June 1982. Two Solid Rocket Boosters (SRBs) were lost (Space Transportation System mission four). The subsequent failure investigation conducted by the National Aeronautics and Space Administration's (NASA) Marshall Space Flight Center (MSFC) indicated that a water impact switch, used to cut the parachutes from the SRBs, functioned prematurely on a spurious shock signal from the SRB frustum separation assembly (FSA). As a result, the parachutes were cut before deployment. The failure investigation prompted three full-scale ground tests of the FSA to be conducted by MSFC.

During test one, the water impact switch remained open. In test three, the switch closed. While in test two, the switch "chattered" but remained open. Approximately 40 channels of shock data were collected in each test. Variations of 50 percent (6 dB) or more were observed for the same measuring location from test to test. These variations raised many questions regarding the repeatability of shock response spectra (SRS) from similar explosive sources and the accuracy and precision of the shock data. These three tests actually raised more questions than they answered.

To date, the single largest problem in studying pyroshocks has been instrumentation. Most companies (past and present) use mounting blocks when mounting accelerometers. These mounting blocks act as mechanical filters; therefore, the data collected are not the actual shock but a response of the mounting block to that shock. In addition, accelerometers are very susceptible to error. Clark [4], DeVorst [5], Keller [6], Sawyer [7], and scores of others have researched accelerometer accuracy, reliability, and error. Errors can range from accelerometer resonance to signal noise, and from lead cable failure to total accelerometer destruction. If these are not enough, consider error input from signal conditioners and amplifiers.

Compared to other areas of technology, pyrotechnic shock technology is still in its infancy. Pyroshocks are nonlinear transient phenomena that have defied mathematical solution and, therefore, remain more of an "art" rather than a "science," being described only by empirical procedures and techniques. Past research efforts have failed to prove if LSC generated SRS are repeatable. Proving shock repeatability for like charges would put this technology one step nearer to a mathematical solution.

The purpose of this project was to analyze variations in pyrotechnically induced shock response spectra and to determine if and to what degree manufacturing and assembly tolerances, distance from the charge, data acquisition instrumentation, and shock energy propagation affect the shock response spectrum. Another major goal of the project was to prove the repeatability of SRS for a given source and to show that these repeatable shocks were higher in level and in frequency than previously believed.

All accelerometers to be used in the test were ball drop calibrated. Next, 28 preliminary plate tests were performed to develop a basic understanding of the shock produced, to evaluate instrumentation, to determine the distance from the source to the accelerometers at which the accelerometers would survive, to determine plate size, and to generally direct the flow of the next plate test series.

The primary plate test series consisted of 36 plates. Variables investigated were core load, plate thickness, alloy variety, standoff, coupling, LSC apex angle, joint effects, mounting block effects, triaxial effects, and combination of variables. Ten shots were used to develop a control case, the base reference mean, and to investigate SRS repeatability.

II. REVIEW OF PREVIOUS PYROSHOCK RESEARCH

Previous LSC pyroshock research has been concentrated into two areas: testing techniques or methods and instrumentation. Various mechanical testing methods have been investigated; however, only live pyrotechnic events are sufficient to produce true pyroshock levels. Due to the violent transient produced by LSCs, instrumentation problems continue to plague test engineers. Before discussing testing techniques and instrumentation, a brief discussion of the most important pyroshock analysis tool, the shock response spectra, is required for general understanding.

A shock response spectrum is defined as a plot of the maximum response of a single-degree-of-freedom system as a function of its own natural frequency in response to an applied shock [8]. Damping is very difficult to determine for shock excited structures. For SRS calculations, damping is always taken at some value between zero and 10 percent. Light damping, less than 10 percent, causes only very slight decreases in SRS levels. Thomson [9] was also used as a basic vibration reference.

There are three types of SRS: primary (response calculated during the shock impulse), residual (response calculated after the shock impulse), and maximax (the maximum response from both primary and residual SRS).

It may be shown mathematically that the theoretical slope of a maximax SRS is 0 dB/octave above a frequency of $f = 1/(2td)$ and 6 dB/octave below $f = 1/(2td)$, where td is the shock impulse time-width. This may be readily seen since the primary spectrum interprets the shock impulse as u(t), a step impulse, while the residual spectrum interprets the shock impulse as $\delta(t)$, a unit impulse.

A. Testing Techniques

With the advent of the space age, many pyroshock testing methods were developed. H. N. Luhrs [10] has one of the better papers summarizing the history of shock testing methods. Early researchers as well as modern researchers have tried unsuccessfully to simulate pyroshock by mechanical means. Bai and Thatcher [11] performed hammer tests that produced desirable SRS, but the time history pulses were too simple, unlike the complex LSC generated pulses. Bell [12] also investigated hammer testing.

Conway [13, 14] and others demonstrated that live charge pyroshock tests could not be simulated using shaker tables. In a similar study, Luhrs [15] demonstrated that shaker tables produce unrealistic test levels even though the SRS may match flight levels. Once again, the time histories were too simple.

Drop testing machines impart a velocity change into a test item, unlike LSCs which induce an acceleration change. Therefore, as a rule, drop testers are not acceptable for pyroshock testing. Fandrich [16, 17] did have limited success with his "bounded impact" technique. However, for LSC induced pyroshock, even this technique does not generate adequate levels.

High intensity shock machines also have demonstrated limited success. Hieber, et al. [1], and Kacena, et al. [2] have shown that for some pyrotechnic devices, not LSCs, similar SRS and time histories are produced.

Hopkinson's Bar, another popular technique, is being used extensively. Neil Davie [18] at Sandia National Laboratory is utilizing this technique on a large scale. Robert Sill [19, 20] is using this technique to calibrate accelerometers. Nilsson [21] also has researched this technique extensively. Once again, the above investigators have demonstrated that mechanically induced shock time histories do not correspond to pyroshock time histories.

Unfortunately, most modern day shock testing involves mechanical simulation techniques, even though researchers in every area of mechanical simulation have shown that mechanical simulation of pyrotechnically induced shock, especially LSC induced shock, is not a valid test method. Past research has shown that explosive shock can only be generated by live explosive testing methods.

The best method of LSC induced pyroshock testing is using the actual flight environment. Obviously, this is not practical except for a few non-critical flight items. Of course, flight data are often, if not always, used to verify ground test techniques. Examples of research using flight data are Engelsferd and Rader [3], Kacena, et al. [2], and scores of others.

The best ground test technique is full-scale testing using actual flight hardware and structures. Keegan and Bangs [22] investigated ground tests to determine effects of various parameters upon spacecraft separation shock. Full-scale ground tests are usually not economically feasible. This leads one to the next best technique, subscale testing. Subscale testing uses a smaller replica of the flight hardware and structure.

Literature indicates that plate testing using live explosives is the best method of simulating spacecraft separation environments where full-scale or subscale flight hardware and structure are not available or are too costly. Lieberman [23, 24] and Powers [25] have indicated that wide variations in SRS have resulted from plate testing.

Another explosive testing technique, barrel testing, is seldom used. Schoessow [26] has proven that the barrel tester gives accurate results if and only if the barrel tester is very similar in structure to the actual flight structure.

Explosive testing is the only way to produce complex shock time histories similar to those generated by LSCs. Plate testing is the most widely used method, probably because of the economics involved in full or subscale ground testing.

B. Instrumentation

Crystal accelerometers are still state-of-the-art for shock measurement. Much work has been done with lasers and fiber optics recently (Kyuma [27]); however, these devices tend to work well only for uni-axial vibration, certainly not pyroshock. There are many problems associated with accelerometers, one must be very careful in choosing these devices. Hicho [28] has an excellent paper describing transducer selection. Piezoelectric and piezoresistive crystal-type accelerometers are used for shock studies because their structural design can survive the high-frequency, high-g environments where other accelerometers fail. High g shock measurement is discussed by Pilcher [29] and piezoshock accelerometry is discussed by Lauer [30], Bouche [31], Kulkarni [32], and Orlacchio [33]. Frederick Schelby [34, 35, 36], Sandia National Laboratories, designs shock accelerometers and shock measurement systems.

Accelerometers are very susceptible to error; accelerometer accuracy, reliability, and error are discussed by Clark [4], Sawyer [7], Keller [6], and DeVorst [5]. Errors can range from accelerometer resonance to signal noise and from lead cable failure to total accelerometer destruction.

Associated with the accelerometers are signal conditioners, amplifiers, and other associated instrumentation. Ball [37] has a paper on signal noise. Purdy [38] worked with piezo accelerometers and their associated instrumentation.

Other types of accelerometer error are test input errors (Marples [39]). One major cause of test input error is accelerometer mounting methodology (Mondshein [40]). If accelerometers are not carefully mounted, high frequency data will be lost or distorted.

Another accelerometer problem is calibration; calibration must be verified for each accelerometer for each test because prominent changes may occur to the crystal during each pyrotechnic event. The Hopkinson's Bar calibration technique is one of the most popular (Sill [20] and Brown [41]). Ball drop calibration is also very popular. Several other techniques exist. Walston, et al. [42] discussed calibration Fourier transform techniques. The following is a list of calibration papers: Brown [43], Bouche [44, 45], Cannon, et al. [46], Clark [47], Ecker [48, 49], Floor [50], Godt [51], Gregory [52], Licht, et al. [53, 54], Macinante [55], Ramboz [56], Webster [57], Wittkowski [58], and Yu, et al. [59].

Errors also occur in data analysis; here it is very important to take multiple trials so that SRS may be verified. Subtle equipment malfunctions will give inaccurate data. Shock response spectra may exhibit a low frequency "hump" due to DC shifting. Many charge amplifiers exhibit DC shifts when encountering large amplitude transients (Schoessow [26]).

Equipment structural design, individual parts sensitivity, and the test method all affect the total test equipment sensitivity and, thus, the pyrotechnic shock spectrum (Luhrs [60]). A majority of data errors can be prevented by carefully selecting data gathering and processing equipment.

Research has proven that tape recorders can clip and distort data. Charge amplifiers can saturate and give erroneous signals. Also, shocks may occur in the resonant range of the accelerometers causing an accelerometer response signal rather than the test component shock signal (Albers [61]). It is better to prevent data errors than to correct them; however, errors occur in even the most carefully designed test setup. Bias terms due to charge saturations and signal errors due to accelerometer resonance can be corrected.

The true signal may be removed from the total or distorted signal (when baseline shifting occurs) by subtracting a bias term as follows:

$$A_{TRUE} = A_{TOTAL} - A_{BIAS} \tag{1}$$

The bias term is defined as follows:

$$A_{BIAS} = A_o \exp[-t/T_o] \tag{2}$$

where

A_o = amplitude of bias

T_o = decaying time constant of bias

t = time

A_o and T_o may be measured from the time history data. When T_o goes to infinity, $A_{BIAS} = A_o$ and a simple direct current shift has occurred.

Accelerometer resonance is a more complicated problem; it may occur at as little as one-tenth the resonant frequency of the accelerometer. Accelerometer response (transfer function) as a function of frequency can be mathematically prescribed if the resonant frequency and damping factor of the accelerometer are known. Accelerometer resonance distortion appears as an amplification of the true signal. A convolution of the real signal with the accelerometer impulse response occurs in real time. The total signal can be deconvolved by Fourier transformation. Then the total signal (now in the frequency domain) may be divided by the accelerometer transfer function to yield the true signal in the frequency domain. The inverse Fourier transform then will yield the true acceleration time history (Moore [62] and Smith [63]).

It is evident from the lieterature that pyrotechnic shock environments are still defined only by empirical procedures. Engelsferd and Rader [3] define guidelines for predicting pyrotechnic environments. These guidelines often prove to be very inaccurate, but they are still considered state-of-the-art. In the last twenty years, instrumentation has improved; however, little progress has been made in defining and predicting pyroshock environments. Another significant problem is within the definition of the SRS. A given SRS is not unique to a given shock transient (a given Fourier spectrum is unique). Most pyroshock simulation tests try to achieve the correct SRS, but more often than not incorrect time histories are produced; therefore, these tests are invalid. A pyrotechnic source should be used instead of a mechanical simulation technique. A pyrotechnic plate test appears to be the best practical test method.

The literature indicates that evidently no one has investigated the effects of LSC manufacturing and charge assembly parameters upon SRS. Also, it is clearly evident that major problems exist in the area of shock test instrumentation. Instrumentation error appears to be the largest single problem in pyroshock research.

III. DESCRIPTION OF EQUIPMENT

Major equipment consists of the test fixture, ball drop calibrator, and signal recording and analyzing equipment. Components such as cables, connectors, switches, etc., will not be discussed. However, support hardware recommended by the accelerometer manufacturers was used.

A. Test Fixture

The test fixture for the main test program consisted of 4 ft x 1 ft x 1/4 in. aluminum plates (plate size was allowed to vary in the preliminary test program). These plates are flat subscale versions of the Space Shuttle SRB frustum and the FSA. The FSA consisted of a 30 grains/ft LSC, charge holder assembly, and charge igniters (all standard SRB equipment). The LSC explosive is cyclotrimethylenetrinitramine (RDX).

The FSA is mounted across the short axis of the test plate; it is bolted onto the plate 3 in. from the end with the cut occurring 2 in. from the end. The accelerometers are mounted upon the opposite end, 2 in. from that end. There is one exception to the accelerometer location; during the joint tests (explained later), one accelerometer is mounted near the charge (FSA).

The test plate assembly (including the FSA) is mounted horizontally upon a wood and steel work table that has been cut out in the center to accommodate the test plate. The plate is suspended by bungee cord (six symmetric pairs along the long side of the plate). The stiffness of the bungee cord was measured to be 2.793 lb/in. The short sides or ends of the test plate are free. At the levels produced by LSC firing, the test plate approaches a free-free state.

Figure 1 is a photograph of the test fixture and its mounting. Figure 2 is a photograph of the charge holder assembly, with linear-shaped charge, mounted onto the test plate. Figure 3 is a drawing of the test fixture.

A series of 28 preliminary tests was conducted to evaluate instrumentation, especially accelerometers, and to gain a general "feel" and understanding of the shock produced. These tests also used 1/4-in. aluminum plates, but the length and width are varied. Also, the LSCs were taped to the plate; no charge holders were used.

Figure 1. The test fixture.

Figure 2. The charge holder assembly.

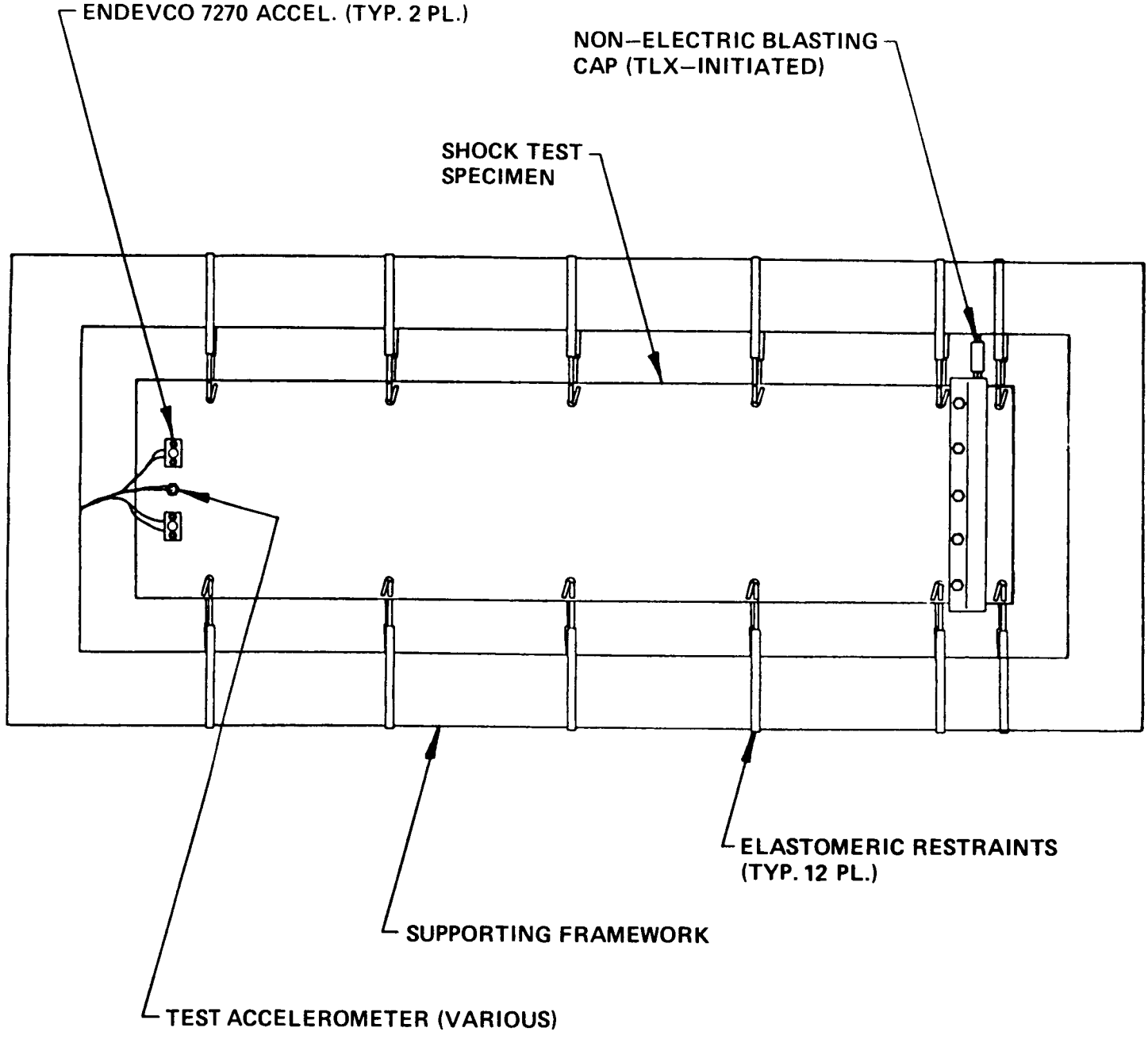

Figure 3. Test fixture drawing.

B. Ball Drop Calibration Apparatus

The ball drop calibrator consisted of a vertical rail upon which a ball holder/dropper and an impact plane holder were mounted. The steel ball weighed 112 grams. It may be dropped manually from the desired height. The ball impacts an anvil upon which the accelerometer to be calibrated is mounted. The accelerometer is mounted below or opposite the impact plane. Four light gates (optical probes) are mounted at 1-in. intervals on the impact holder below the impact plane. The accelerometer anvil assembly is mounted in a block, so that upon impact it may fall freely. The ball and anvil fall through the light gates to a foam catch tray below. Figure 4 illustrates the ball drop apparatus. Figure 5 illustrates the ball release mechanism. Figures 6 and 7 show the impact plane, impact anvil, and accelerometer. Below the impact plane the optical probes are shown.

C. Signal Recording and Analyzing Equipment

Seven varieties of accelerometers were used in the test program. Donald Baker Moore [64] of Explosive Technology summarized the characteristics of these accelerometers in Figure 8. This information originally came from product literature.

Figure 9 illustrates the shock test setup from an instrumentation standpoint. The firing unit triggers the igniter, firing the LSC in the FSA, thus severing the test plate. The shock test is recorded visually by the television camera and tape machine (VHS cassette). A time generator annotates the video recording. The voltage signals from the accelerometers travel by cable to the signal processing instrumentation.

Figure 10 illustrates the signal recording and processing instrumentation. The instrument system is controlled by the HP9816 computer. Within the system are digital storage oscilloscopes, digital memories, regular oscilloscopes, etc. The two most important data processing instruments are the Spectral Dynamics (SD) SD320 Shock Spectrum Analyzer and the SD375 Fast Fourier Transform Signal Analyzer. Scientific Atlanta manufactures SD instruments.

The SD320 STS analyzer uses the raw analog time histories, converting them into frequency response plots. Electronically simulated simple harmonic oscillators at each frequency bandwidth from 0 to 10,000 Hz are exposed to the shock impulse, producing the final SRS. A 100,000 Hz SRS may be produced by reducing the input signal speed, so that the SD320 thinks the 100,000 Hz data is 10,000 Hz data. This procedure has been laboratory verified.

The SD375 uses analog time histories also. Dual or single channel analysis is possible up to 1,000,000 Hz. The SD375 is capable of real time analysis. Several system functions may be computed and displayed for one or both channels.

Figures 11 and 12 are photographs of the accelerometers mounted upon the test plate and the data recording and analyzing instrumentation.

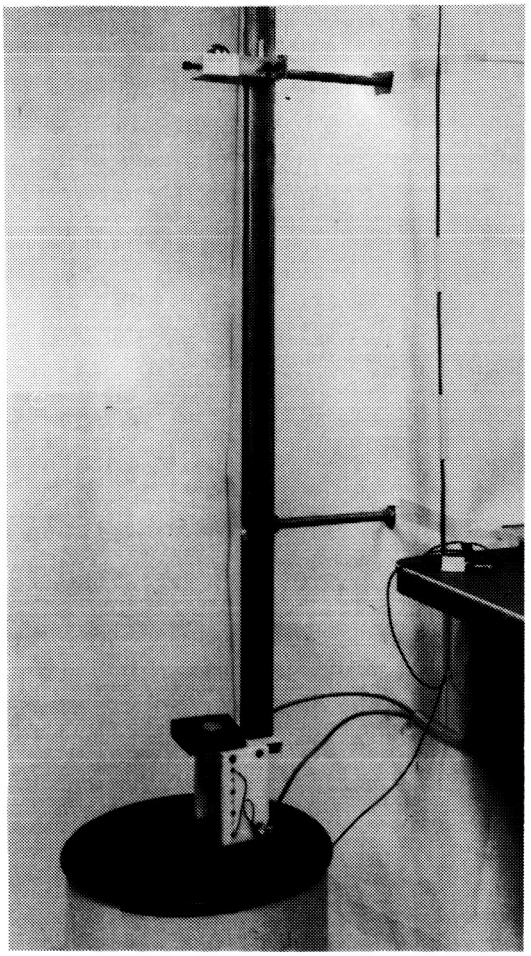

Figure 4. The ball drop apparatus.

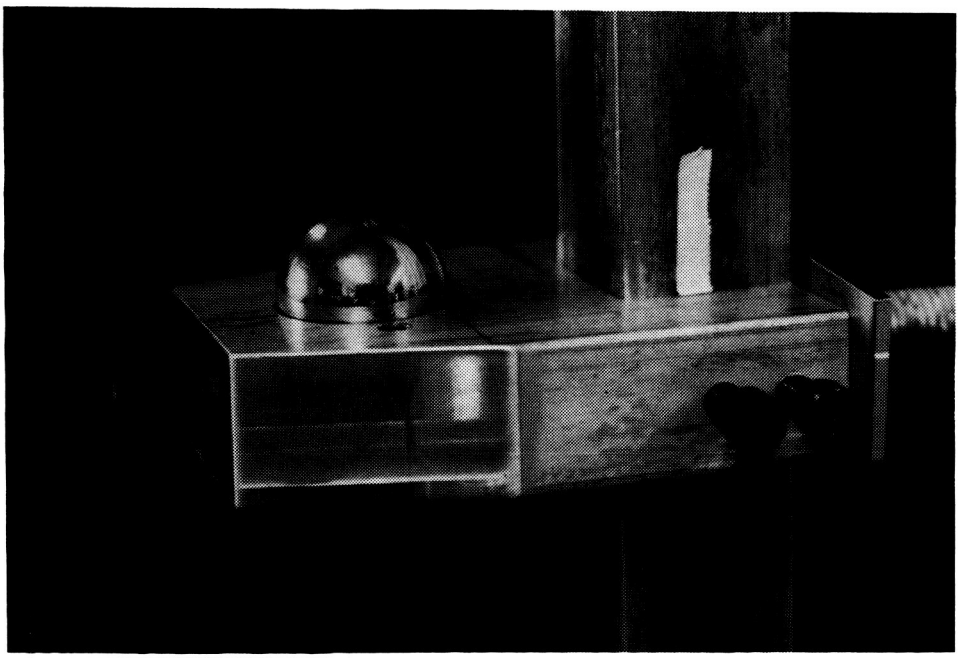

Figure 5. The ball release mechanism.

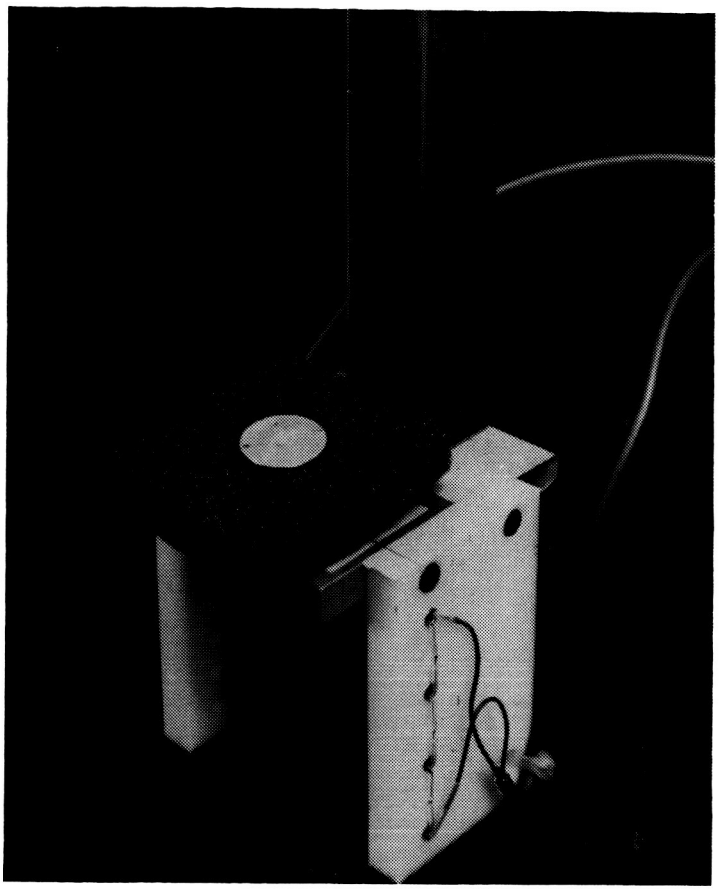

Figure 6. The impact plane.

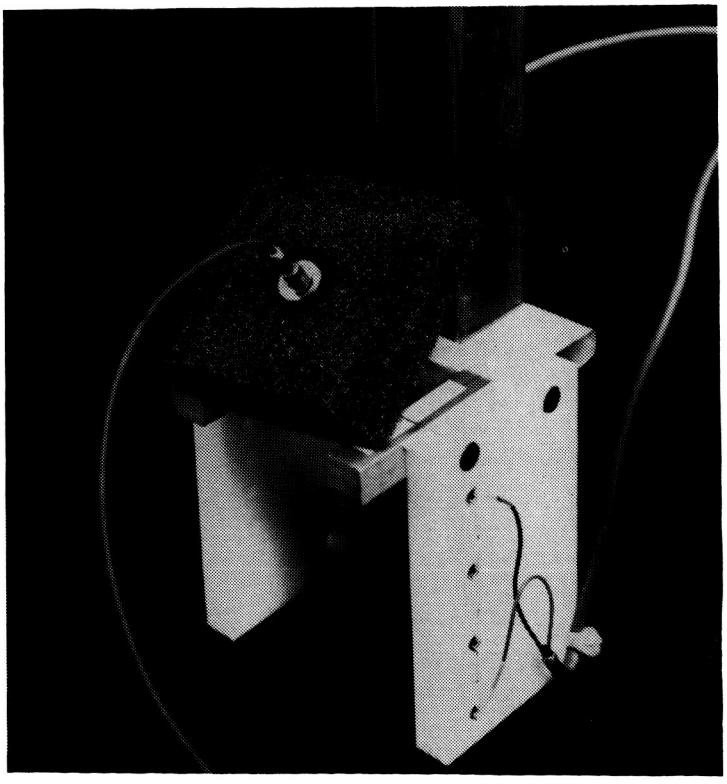

Figure 7. The impact plane.

ACCELEROMETER CHARACTERISTICS	ENDEVCO 7270	ENDEVCO 2225	KISTLER 805B	B & K 8309	PCB 305A	DYTRAN 3200A	ENDEVCO 2291
WEIGHT, GRAMS	1.5	13	8	5.1	7	12	1.3
SENSITIVITY	1-3 μV/g	.65mV/g	.05pC/g	.004pC/g	.5mV/g	.05mV/g	.01mV/g
RANGE, g's	±200,000	±20,000	+100,000 –50,000		±100,000	±100,000	±100,000
FREQUENCY RESPONSE, Hz	100 – 100,000	5 – 15,000	1 – 12,000	1 – 54,000			20 – 50,000
RESONANT FREQUENCY, KHz	1,300	80	70	180	60	300	250

Figure 8. Accelerometer characteristics table.

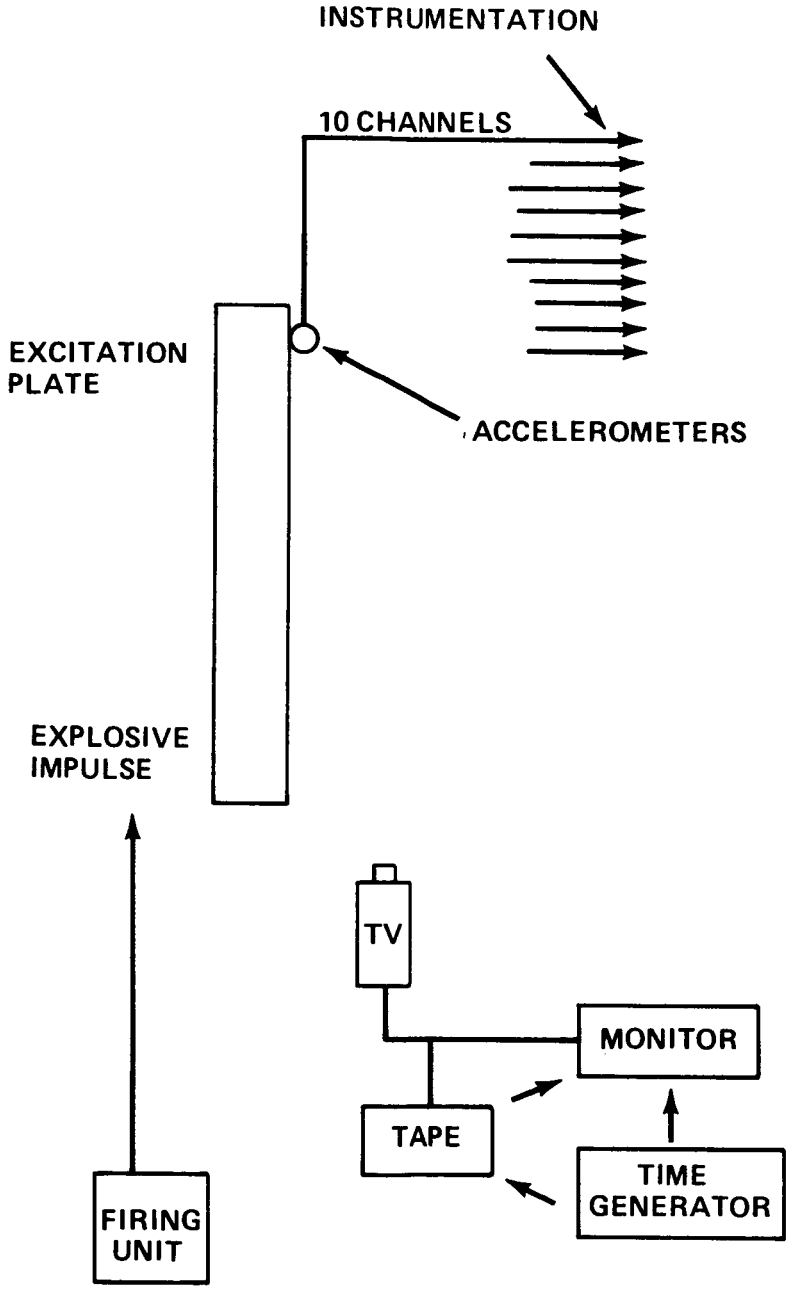

Figure 9. Shock test setup – instrumentation.

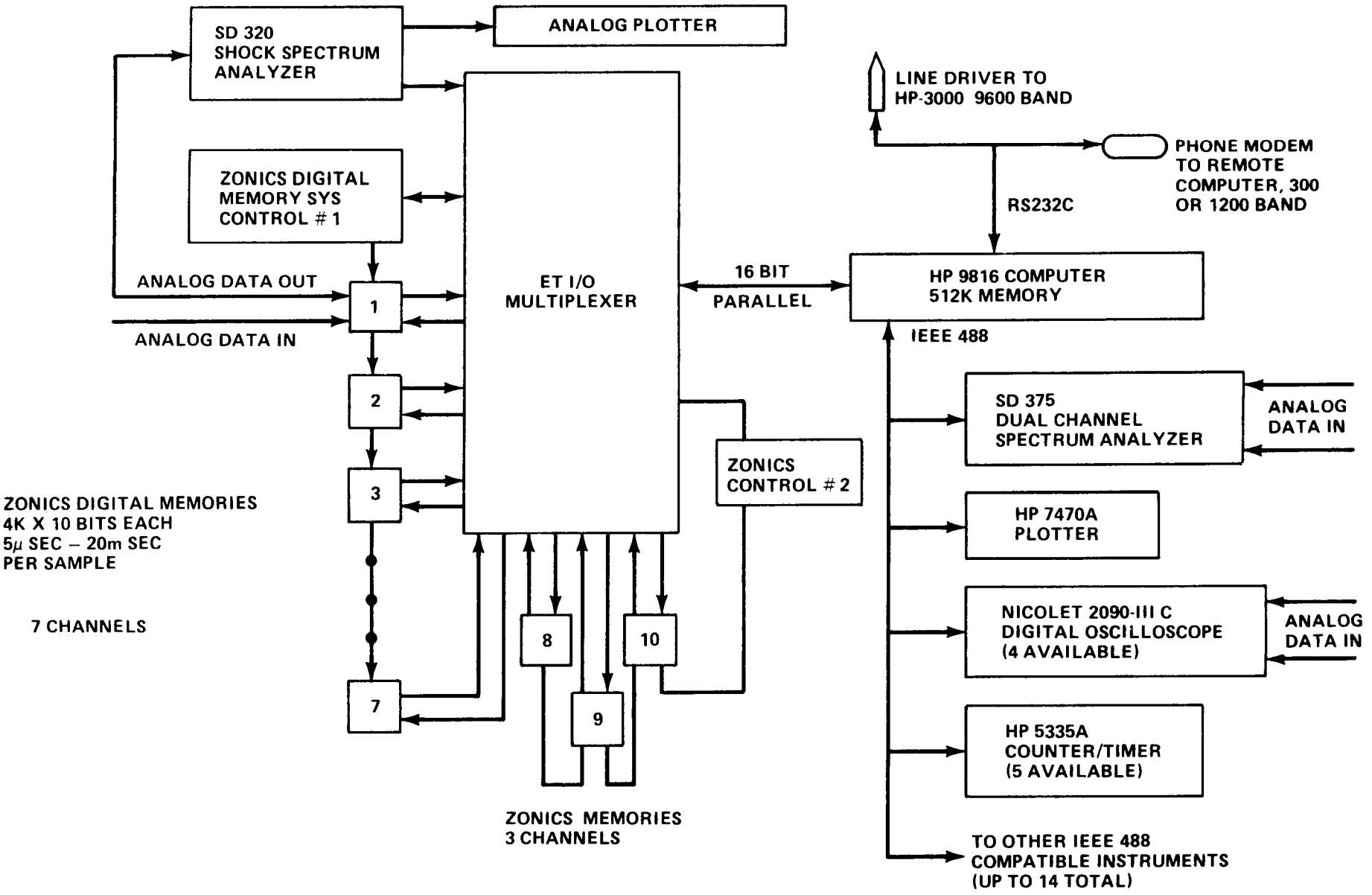

Figure 10. Signal recording and processing instrumentation.

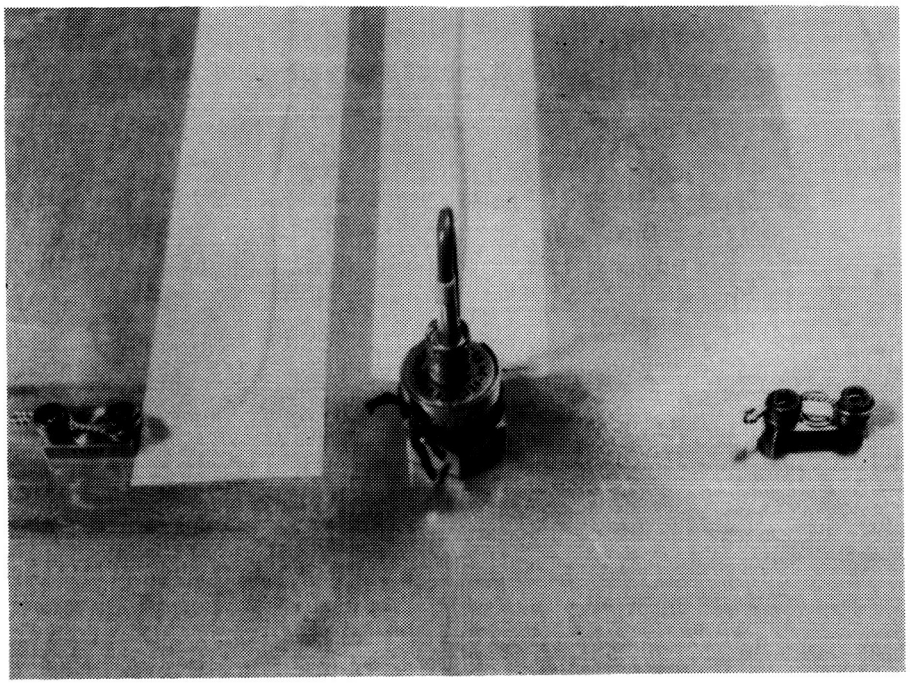

Figure 11. Mounted accelerometers.

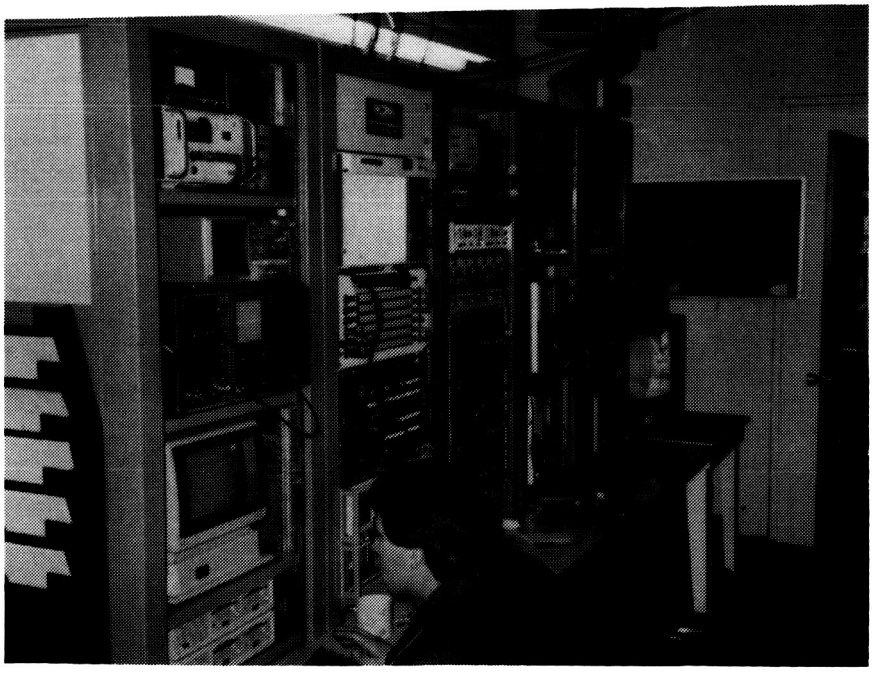

Figure 12. Instrumentation panel.

IV. EXPERIMENTAL PROCEDURES

This section describes the various variables investigated and the techniques used to obtain shock data. Testing consisted of a series of preliminary tests, basic shock spectra tests (control case), and variability tests (experimental case). Ball drop calibration and plate tests were used throughout the program.

A. General Procedures

Ball drop calibration techniques, plate test techniques, and standard firing procedure are outlined in the following three subsections.

1. Ball Drop Calibration

Accelerometer sensitivity may be evaluated by using the ball drop calibrator described in the previous section. A ball is dropped from a specified height onto the impact anvil which contains the accelerometer. Calibration is accomplished by integrating the acceleration time signal from the accelerometer to obtain the velocity estimate. This estimate is then compared with the nominal resultant velocity of the ball-anvil mass assuming no ball rebound and conservation of momentum, or the actual velocity of the anvil as measured by displacement versus time from the light gates. These measurement variables were also considered. The anvil was used plain, with one layer of electrical PVC tape, and with two layers of PVC tape on the impact surface. This tape insured no ball rebound.

2. Plate Test

Plate tests were used as the primary test technique. First, the test fixture is set up as outlined previously. The plate is severed by initiating the charge using standard firing procedure. The time history of the shock transient is captured by three accelerometers and recorded on disc and the digital memories. Real time Fourier analysis is accomplished. The time histories are captured using 4-, 20-, and 200-millisecond windows. The 4-millisecond window is used to derive the high-frequency shock spectra, the 20-millisecond window is used to derive the low-frequency shock spectra, and the 200-millisecond window is used to record the entire event. All SRS data are maximax with a Q of 10 or 5 percent damping.

3. Standard Firing Procedure

The firing procedure utilized in this program is outlined in the Explosive Technology Standard Test Firing Panel, PN80012, Operating Procedure manual.

B. Precision and Accuracy

First, the accelerometers and associated instrumentation were ball drop calibrated using a steel anvil and then an aluminum anvil. Then, 28 preliminary test shots were made to evaluate proper plate size, instrumentation capabilities, and effects of initiation methods upon shock. Eleven accelerometer types from five manufacturers were evaluated. Twenty shots were made with thirty grain RDX LSCs and eight shots were made with blasting caps only. Twenty-one tests used electric blasting caps, and

seven used non-electric blasting caps to investigate possible effects of electrical interference from the electric caps upon the accelerometers. This test program was an informal preliminary test series designed to establish a "feel" for the equipment, the test apparatus, and the shock environment produced. Various plate sizes were used, but all plates were 1/4-in. thick. Based upon these tests, accelerometers were chosen for the final or main test program, based upon survivability and accuracy of data. Also, these tests determined the plate size and the distance of the accelerometers from the source. Precision and accuracy were evaluated further by including two 7270 accelerometers and one variable (experimental) accelerometer on most plate tests in the main test program.

C. Basic Shock Response Spectra

Ten plate tests were performed using procedures previously outlined. Very close attention was given to the LSC geometry to ensure that it was as nearly perfect as possible. The object of these tests was to have no variables in the LSC or its mounting. There were two variables in these ten tests. Five plates had aluminum alloy 6061-T6 and five had aluminum alloy 2219-T87. Four plates did not have the target area slot; the other six plates did have the slot as well as all remaining plates. Figure 13 is the actual test matrix showing the variables, accelerometers, etc., for each shot. It was believed that alloy type would not affect the SRS. Also, it was believed that the target slot would not affect the SRS as long as the plate was severed. Thus, the ten shocks produced should be very reproducible or repeatable. These shots will establish a base reference mean SRS or a control case for comparison in the variability tests. If alloy or plate thickness had indeed varied the SRS, the remaining shot scheduled would have been revised.

D. Variability

Twenty-six plate tests were conducted using procedures previously outlined. Variables included coreload, standoff, coupling, jointed plate, combination of coreload, standoff, and coupling based upon effects of each individually, LSC apex angle, accelerometer mounting, gross variation in coreload, and triaxial comparison. Figure 13, the shot matrix, lists these tests as shots 11 through 36. The values for the variables, minimums and maximums, are based upon NASA specifications and quality control standards.

V. DATA ANALYSIS AND RESULTS

The test program was subdivided into three general areas: precision and accuracy, basic shock response spectra, and variability. Precision and accuracy contains the ball drop calibration tests, the preliminary plate test series, and the accelerometer and instrumentation evaluation from all the tests. Within the basic shock response spectra section are the first ten plate tests of the primary test series. Alloy variety and target thickness are evaluated; also, the average or basic shock response spectra (control case) for the system is derived. Comparisons are made between the basic SRS and the predicted SRS. Finally, the variability area includes the remaining tests of the primary plate test series where manufacturing and assembly variables were evaluated and supplementary studies were performed.

SHOT NUMBER	TARGET THICKNESS (IN.)	ALLOY	PURPOSE	PARAMETER	VALUE	VARIABLE ACCELEROMETER (3)
1	0.250	TEST (1)	BASE	NONE	NONE	2291
2	0.250	TEST	REFERENCE	NONE	NONE	2291
3	0.250	DESIGN (2)	SHOCK	NONE	NONE	2255A
4	0.250	DESIGN (2)	RESPONSE	NONE	NONE	2255A
5	0.215	TEST	SPECTRA	NONE	NONE	DYTRAN 3200A
6	0.215	TEST	SPECTRA	NONE	NONE	B & K 8309
7	0.215	TEST	SPECTRA	NONE	NONE	KISTLER 805B
8	0.215	DESIGN	SPECTRA	NONE	NONE	KISTLER 805B
9	0.215	DESIGN	SPECTRA	NONE	NONE	DYTRAN 3200A
10	0.215	DESIGN	SPECTRA	NONE	NONE	B & K 8309
11	0.215	TEST	PARAMETRIC	CORELOAD	MAX.	2255B
12	0.215	TEST	EFFECTS	CORELOAD	MAX.	2255B
13	0.215	TEST	EFFECTS	CORELOAD	MIN.	B & K 8309
14	0.215	TEST	EFFECTS	CORELOAD	MIN.	B & K 8309
15	0.215	TEST	EFFECTS	STANDOFF	MAX.	KISTLER 805B
16	0.215	TEST	EFFECTS	STANDOFF	MAX.	KISTLER 805B
17	0.215	TEST	EFFECTS	STANDOFF	MIN.	2255B
18	0.215	TEST	EFFECTS	STANDOFF	MIN.	2255B
19	0.215	TEST	EFFECTS	COUPLING	MAX.	DYTRAN 3200A
20	0.215	TEST	EFFECTS	COUPLING	MAX.	DYTRAN 3200A
21	0.215	TEST	EFFECTS	COUPLING	MIN.	2255B
22	0.215	TEST	EFFECTS	COUPLING	MIN.	2255B
23	0.215	TEST	EFFECTS	(JOINT IN PLATE) (4)	(3 INCH OVERLAP)	7270
24	0.215	TEST	EFFECTS			NONE
25	0.215	TEST	EFFECTS	(COMBINATION OF COUPLING CORELOAD AND STANDOFF)	MIN.	NONE
26	0.215	TEST	EFFECTS		MIN.	NONE
27	0.215	TEST	EFFECTS		MAX.	NONE
28	0.215	TEST	EFFECTS		MAX.	NONE

Figure 13. Test shot schedule.

SHOT NUMBER	TARGET THICKNESS (IN.)	ALLOY	PURPOSE	PARAMETER	VALUE	VARIABLE ACCELEROMETER (3)
29	0.215	TEST	EFFECTS	LSC APEX ANGLE	MIN.	NONE
30	0.215	TEST	EFFECTS	LSC APEX ANGLE	MAX.	NONE
31	0.215	TEST	EFFECTS	ACCELEROMETER MOUNTING	BLOCK vs. FLAT	7270
32	0.215	TEST	EFFECTS	ACCELEROMETER MOUNTING	BLOCK vs. FLAT	7270
33	0.215	TEST	EFFECTS	TRIAXIAL RESPONSE	X vs Y vs Z AXES	7270
34	0.215	TEST	EFFECTS	TRIAXIAL RESPONSE	X vs Y vs Z AXES	7270
35	0.215	TEST	EFFECTS	GROSS VARIATION IN CORELOAD	25 GRAIN	2255B
36	0.215	TEST	EFFECTS	GROSS VARIATION IN CORELOAD	40 GRAIN	2225, 2255B

(1) TEST ALLOY = ALUMINUM 6061–T6

(2) DESIGN ALLOY = ALUMINUM 2219–T87

(3) ENDEVCO ACCELEROMETERS UNLESS OTHERWISE NOTED. TWO ENDEVCO 7270 ACCELEROMETERS WERE USED IN EACH SHOT WITH A THIRD VARIABLE ACCELEROMETER FROM VARIOUS COMPANIES BEING ADDED FOR ACCELEROMETER EVALUATION.

(4) TEST SHOT #23 ALSO INCLUDED ONE 7270 ON A MOUNTING BLOCK.

NOTES: RECORDING TIMES OF 4, 20, AND 200 MILLISECONDS WERE USED FOR EACH SHOT. THE FOUR MILLISECOND WINDOW WAS USED TO DERIVE THE HIGH FREQUENCY SPECTRA, THE 20 MILLISECOND WINDOW FOR THE LOW FREQUENCY SPECTRA, AND THE 200 MILLISECOND WINDOW TO RECORD THE ENTIRE EVENT.

ONE FEET BY FOUR FEET TEST PLATES WERE USED FOR ALL SHOTS EXCEPT #23 AND #24. IN THESE THE PLATE WAS SEVERED TEN INCHES FROM THE FSA END. THEN THE PLATES WERE JOINTED WITH A THREE INCH OVERLAP AND FIVE FSA BOLTS – THIS RESULTED IN THE PLATE BEING THREE INCHES SHORTER.

THE PLATE THICKNESS FOR ALL SHOTS WAS .25 INCHES. HOWEVER, ALL PLATES EXCEPT SHOTS # 1, 2, 3, AND 4 WERE SLOTTED IN THE FSA TARGET AREA TO IMPROVE SEVERABILITY. PRELIMINARY TESTS INDICATED THAT 30 GRAINS/FOOT RDX WOULD NOT SEVER .25 INCH ALUMINUM PLATE.

Figure 13. (Concluded)

A. Precision and Accuracy

The first portion of the precision and accuracy program consisted of ball drop calibration tests. First, the optical sensors were checked by dropping the 112-gram steel ball through the light sensors with the impact platform removed. A height of 32.350 in. was used. All free fall velocities were accurate with the theoretical within 0.5 percent. The measured velocities were 13.15 ± 0.05 ft/sec. The predicted or theoretical velocity assuming free fall and no air friction was calculated as follows:

$$V_{BALL} = \sqrt{2gh} = 13.150 \text{ ft/sec}$$

where

$h = 32.250$ in.

$g = 32.174 \text{ ft/sec}^2$.

Next, each accelerometer was ball drop calibrated using a steel anvil (49 grams) and then repeated using an aluminum anvil (17 grams). Each test was repeated three times, once with a bare anvil, once with one layer of PVC electrical tape on the anvil, and once with two layers of PVC tape on the anvil. The electrical tape was used to make the ball-anvil collision more inelastic. From each test, the accelerometer response and the light sensor response were recorded. These were compared with the predicted or theoretical velocities. Assuming conservation of momentum and inelastic impact, the velocity of the coupled ball-anvil mass may be calculated as follows:

$$V_f = \frac{M_{BALL} \cdot V_{BALL}}{M_{BALL} + M_{ANVIL} + M_{ACCELEROMETER}}$$

where

V = velocity

M = mass .

Figure 14 shows the results of the calibration tests and theoretical predictions.

Comparisons were made between accelerometer measurements and theoretical predictions, and then between accelerometer measurements and light sensor measurements. It was observed that the accelerometer leads protruded below the mounting platform, thus interfering with optical sensors by blocking or interrupting the light path. Also, it was evident that the ball-anvil collision was still not completely inelastic. A final ball drop test series was instigated using putty on the anvil surface to insure an inelastic collision.

The accelerometer (Endevco 7270) measured a velocity of 8.40 ft/sec. The predicted velocity, allowing for the mass of the putty, was 8.69 ft/sec. The accuracy was 96 percent. With the putty, the

VELOCITIES (FT/SEC)

	ACCELEROMETER	ENDERCO 7270	ENDERCO 2225	KISTLER 805B	B & K 8309	PCB 305A	DYTRAN 3200A	ENDERCO 2291
STEEL ANVIL	THEORETICAL	9.06	8.46	8.72	8.87	8.78	8.51	9.07
	NO TAPE ACCELEROMETER	14.10	13.76	14.40	15.20	11.84	12.96	13.76
	NO TAPE LIGHT SENSOR	17.60	15.40	17.40	24.00	18.40	18.20	20.70
	1 LAYER ACCELEROMETER	8.96	9.28	9.92	10.24	8.00	8.40	9.12
	1 LAYER LIGHT SENSOR	7.20	13.20	7.20	12.80	13.80	8.00	6.90
	2 LAYERS ACCELEROMETER	8.90	8.64	9.92	10.48	8.00	8.00	10.80
	2 LAYERS LIGHT SENSOR	4.60	5.20	5.60	7.20	5.60	4.80	6.40
ALUMINUM ANVIL	THEORETICAL	11.29	10.37	10.75	10.98	10.83	10.45	11.30
	NO TAPE ACCELEROMETER	16.00	14.40	16.84	17.60	14.72	14.08	15.68
	NO TAPE LIGHT SENSOR	19.60	12.00	17.60	23.00	16.80	14.40	19.20
	1 LAYER ACCELEROMETER	13.20	13.44	13.44	14.40	12.80	13.24	14.00
	1 LAYER LIGHT SENSOR	13.60	8.80	12.80	15.20	13.30	11.20	12.00
	2 LAYERS ACCELEROMETER	12.48	11.52	14.00	14.08	12.48	11.84	12.48
	2 LAYERS LIGHT SENSOR	8.40	7.60	10.00	10.80	10.40	8.80	8.80

Figure 14. Ball drop calibration data.

calibration was accurate within 4 percent (a high degree of accuracy for shock measurement). The Hopkinson's Bar was clearly a better method but one was not available for this study.

Next, a series of 28 preliminary plate tests were performed. The results of the plate tests were used to direct the flow of the main test program. Results indicated (after destroying several accelerometers) that the plate size should be modified from 48 in. x 24 in. x 0.25 in. to 48 in. x 12 in. x 0.25 in. Originally, the cut was to be made in the center of the plate through the short axis. However, preliminary results demonstrated that to insure moderate accelerometer survival, the accelerometers should be at least 40 in. from the source. To accomplish this, the plate would have to be cut across one end, with the accelerometers mounted across the other end. Finally, preliminary results indicated that the Endevco 7270 accelerometer demonstrated the highest degree of survivability and the lowest degree of baseline shifting; therefore, it was chosen as the primary accelerometer. However, other accelerometers were used for evaluation purposes on all plate tests. The preliminary plate tests also provided a general idea of the time histories and SRS to be expected in the main test program. Also, during the preliminary tests, the initiation method (electric versus non-electric blasting caps) was evaluated. It was found that this variable did not affect the SRS. Many experts had believed that electrical noises from the electric blasting caps might affect the accelerometers. However, as a precaution, non-electric caps were used in the primary test program.

After the entire test program was completed, a separate analysis was made of the primary test program data to further evaluate accelerometers and associated instrumentation. Figure 15 summarizes the survivability and baseline shifting of the accelerometers, located 40 in. from the source.

ACCELEROMETER VARIETY	NUMBER OF CHANNELS	NUMBER OF TOTAL FAILURES	BASELINE SHIFTS	ACCELEROMETER RESONANCES	GOOD DATA
ENDEVCO 2291	2	0	2	2	0
ENDEVCO 2255A	2	0	2	1	0
DYTRAN 3200A	4	1	2	2	1
B & K 8309	4	0	4	3	0
KISTLER 805B	4	0	3	2	1
ENDEVCO 2255B	8	0	7	6	1
ENDEVCO 2225	1	0	0	0	1
ENDEVCO 7270	77	*7	4	0	66

*NOTE: SIX OF THESE FAILURES WERE ATTRIBUTABLE TO AMPLIFIER PROBLEMS AND OTHER FORMS OF INTERFERENCE. ONLY ONE FAILURE WAS DUE TO INTERNAL ACCELEROMETER FAILURE.

Figure 15. Accelerometer failure statistics.

Figures 16 and 17 are time history traces from Endevco 7270 and 2291 accelerometers, respectively, side by side measurements from the same test. Note that the 2291 trace appears to be amplified and slightly baseline shifted upward. Figures 18 and 19 are 0 to 400,000 Hz Fourier transforms for the time traces. Notice the 2291 resonates around 260,000 Hz, the signal is also amplified below 40,000 Hz. These are the types of problems encountered in shock accelerometry. The 7270 was the only accelerometer resonance during the tests. Only 7270 data were used for the primary tests data analysis.

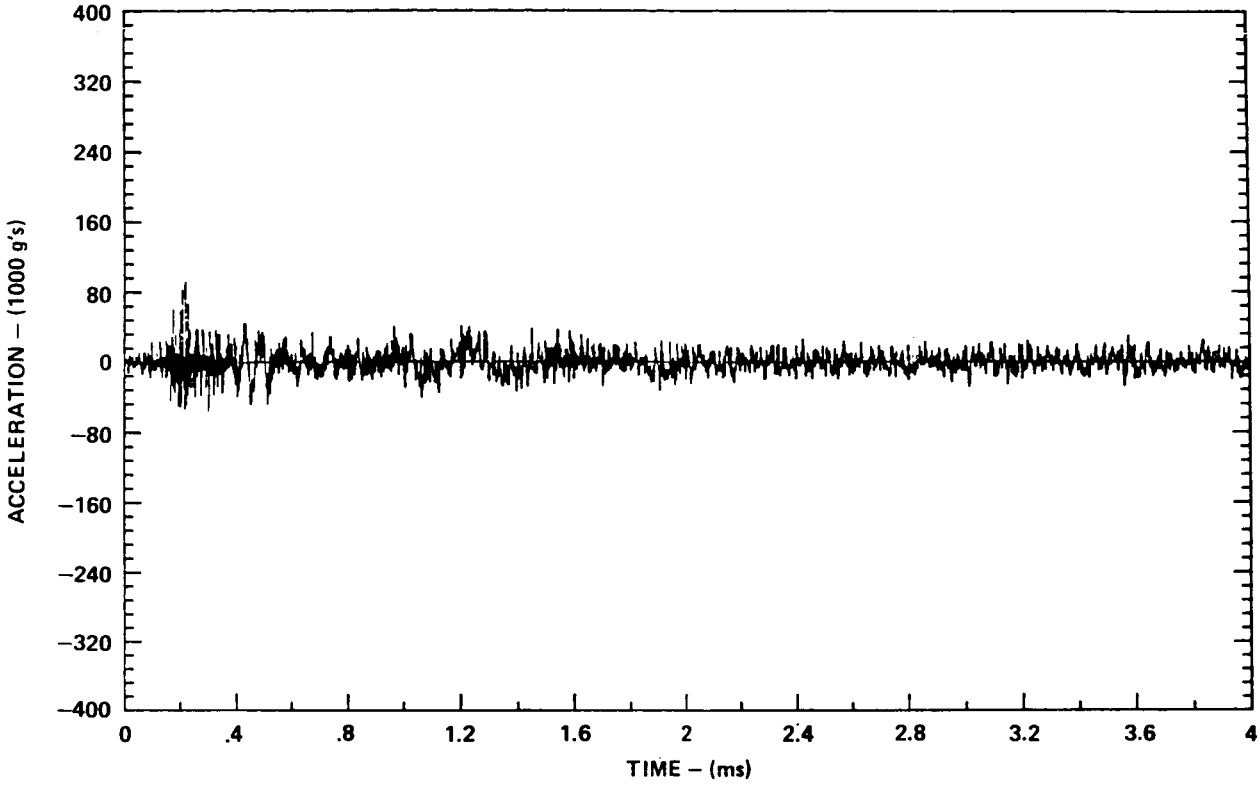

Figure 16. Acceleration time history.

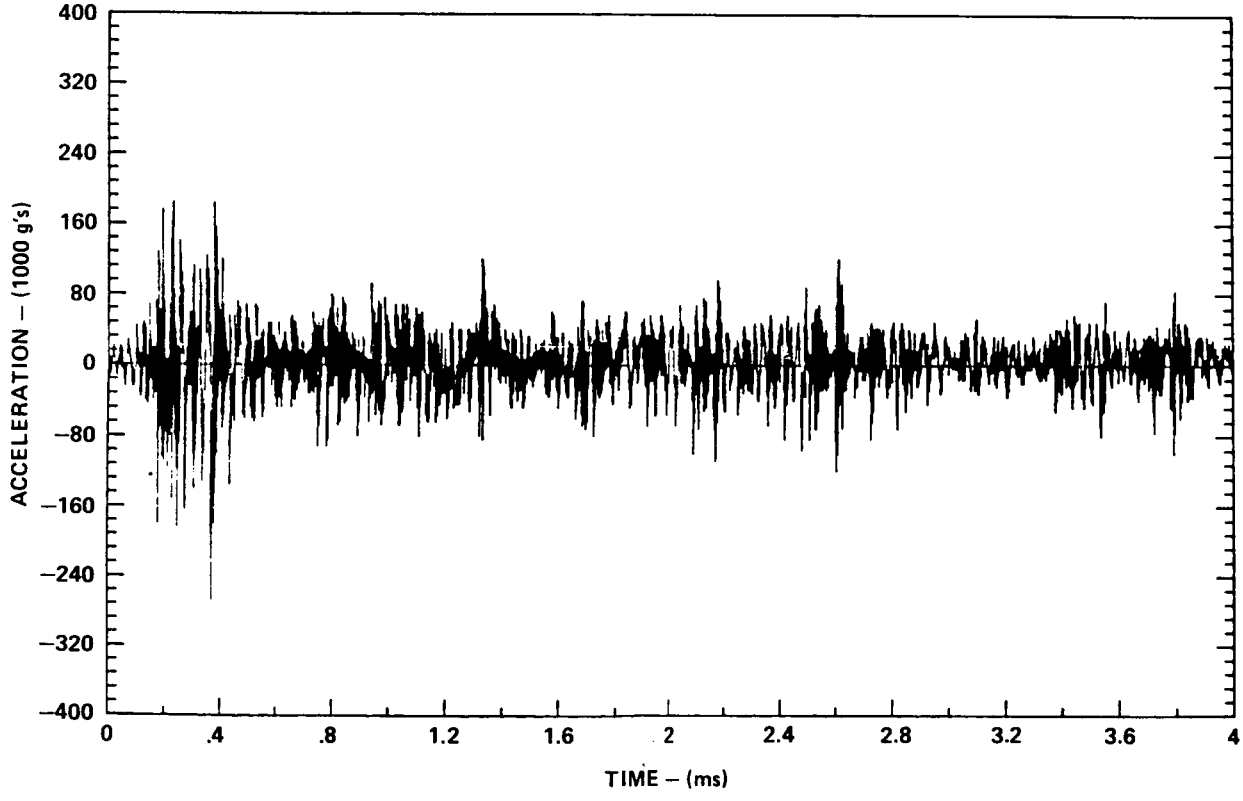

Figure 17. Acceleration time history.

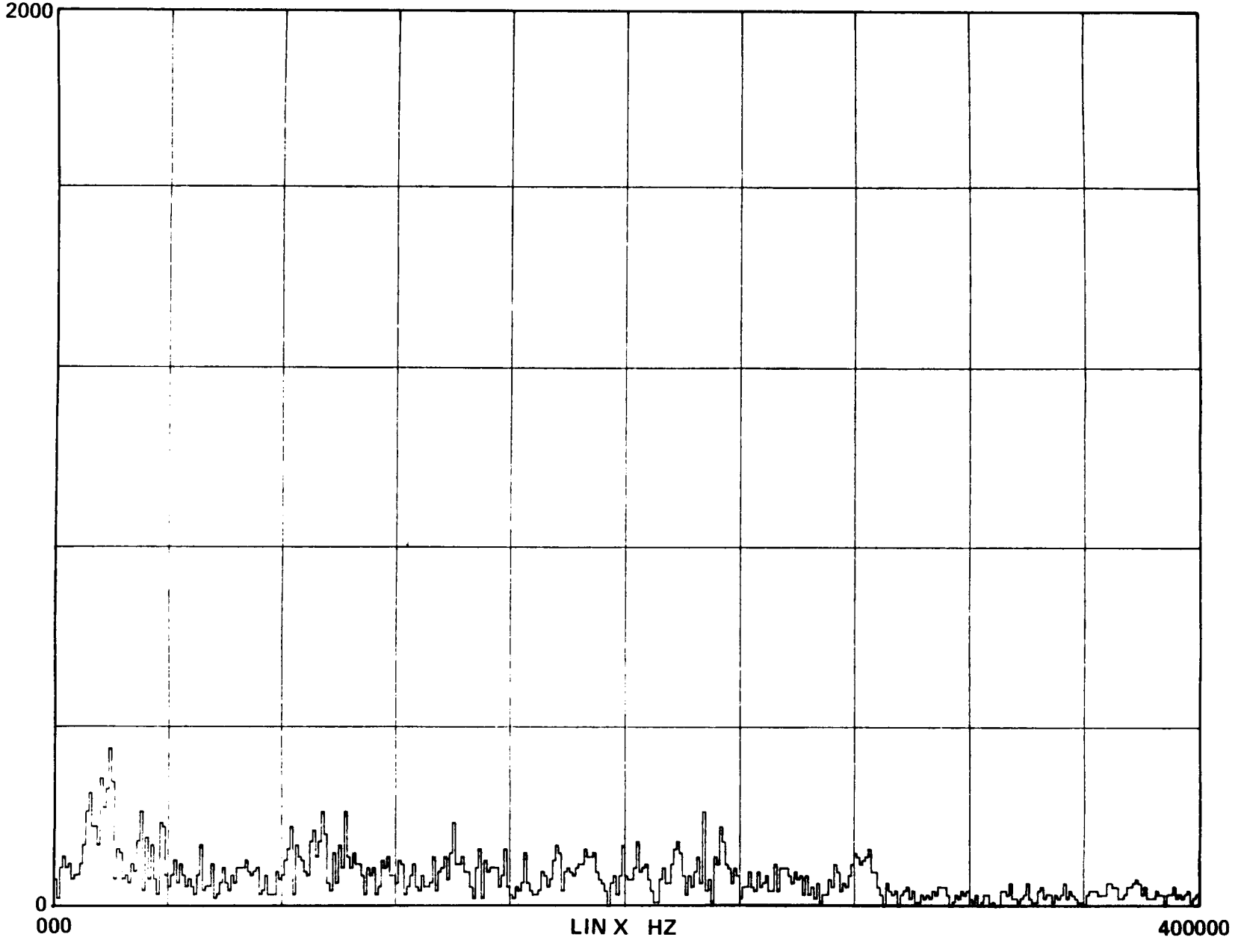

Figure 18. Fourier transform.

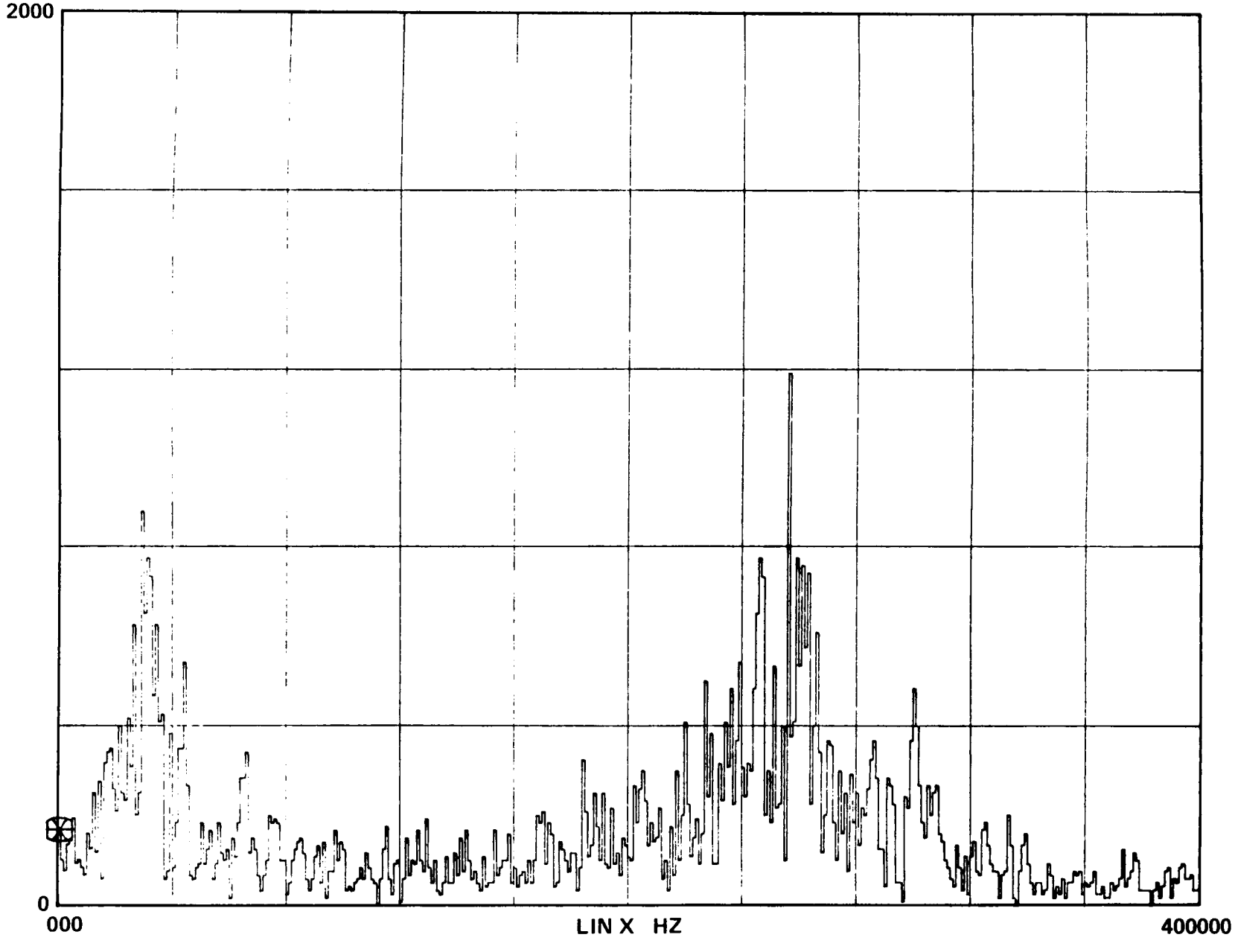

Figure 19. Fourier transform.

In addition to baseline shifts and accelerometer resonances, erratic levels were recorded on many accelerometers. Figure 20 is a bar graph representing the peak g's recorded during the first 10 plate tests (control case), where the base reference mean was established. The lowest peak g level and the highest peak g level are noted for each accelerometer. The dotted line represents the base reference mean level. Figure 21 is an envelope of the 9 test accelerometer SRS and the 7270 accelerometers from the first 10 plate tests. Figure 22 compares the base reference mean SRS from the 7270 with the mean SRS derived from the 9 test accelerometers. Note, the "baseline shift" is very evident between 10 and 4000 Hz. The error between the other accelerometers and the 7270 is presented as decibel (dB) variation in Figure 23. This error function in dBs as a function of frequency can be represented by an equation. Utilizing a computer graphics program and recognizing the general shape of the error data, constants were chosen for the following distribution:

$$Y = C_1 + [C_2(X-C_3)\exp(C_4(X-C_3)^2)] \quad .$$

Constants were derived by trial and error using the graphics program. Y is the dB_{ERROR} and X is the $\log_{10}f$ since our data is plotted in semilog coordinates. The resultant equation is as follows:

$$dB_{ERROR} = 2.12 + [34.81(F)\exp(-0.6173(F)^2)]$$

where $F = (\log_{10}f)-0.9$. The large error in Figure 23 clearly illustrates how much variation may occur in SRS due to instrumentation.

B. Basic Shock Response Spectra

In order to evaluate the variables associated in manufacturing and assembly of LSCs and the FSA, a control case was needed for comparison. Normally, a control test does not include any variables. In these tests (the first 10 plate tests of the primary program), two variables were considered because previous tests indicated that these two variables would not vary the SRS. The two variables were aluminum alloy and target thickness. The design alloy of the FSA was aluminum 2219-T87; this alloy is a special order item and only a few sheets were available (not enough for the test program). Aluminum alloy 6061-T6 (henceforth referred to as test alloy) was readily available. Preliminary analysis indicated that all alloys of aluminum would respond in the same manner, not affecting SRS. Five plates in this phase were design alloy and five were test alloy. It should be noted that only 7270 data were used for basic shock response spectra analysis, due to the error induced by other accelerometers as explained previously.

Target thickness involved slotted and unslotted test plates. Once again, preliminary analysis indicated that 30 grain/ft RDX LSC would not sever 1/4-in. plates. Common practice is to slot the plates in the target area. Four plates were unslotted, all remaining plates had slots resulting in a target thickness of 0.215 in. The idea was to investigate incomplete versus complete plate severance. However, all plates were cleanly severed. Means and envelopes were calculated for all 10 tests and combinations of tests.

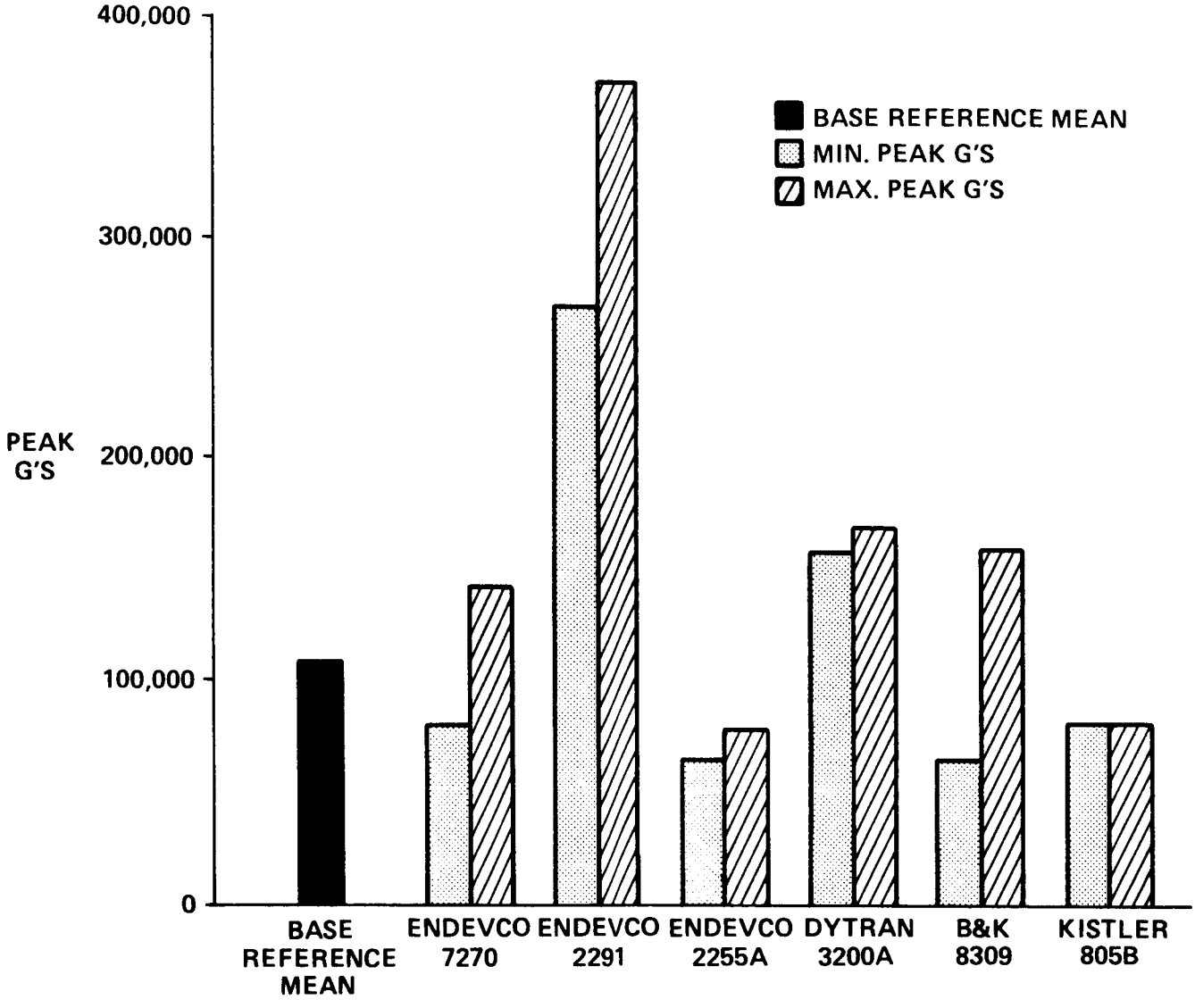

Figure 20. Accelerometer variation – peak g's for control case (shots 1 through 10).

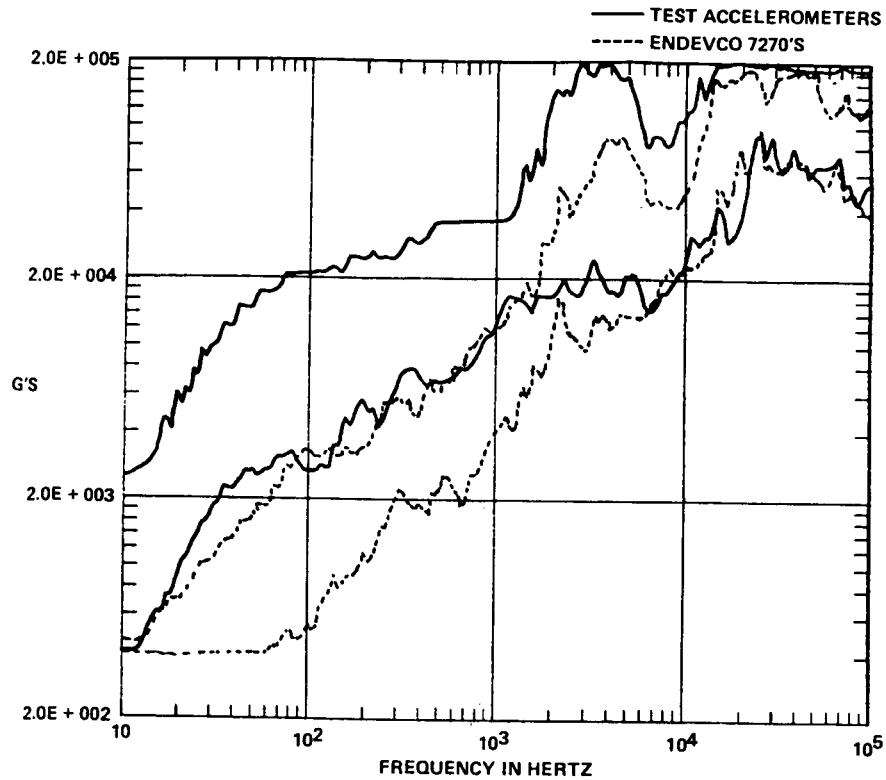

Figure 21. SRS envelopes: test accelerometers versus Endevco 7270.

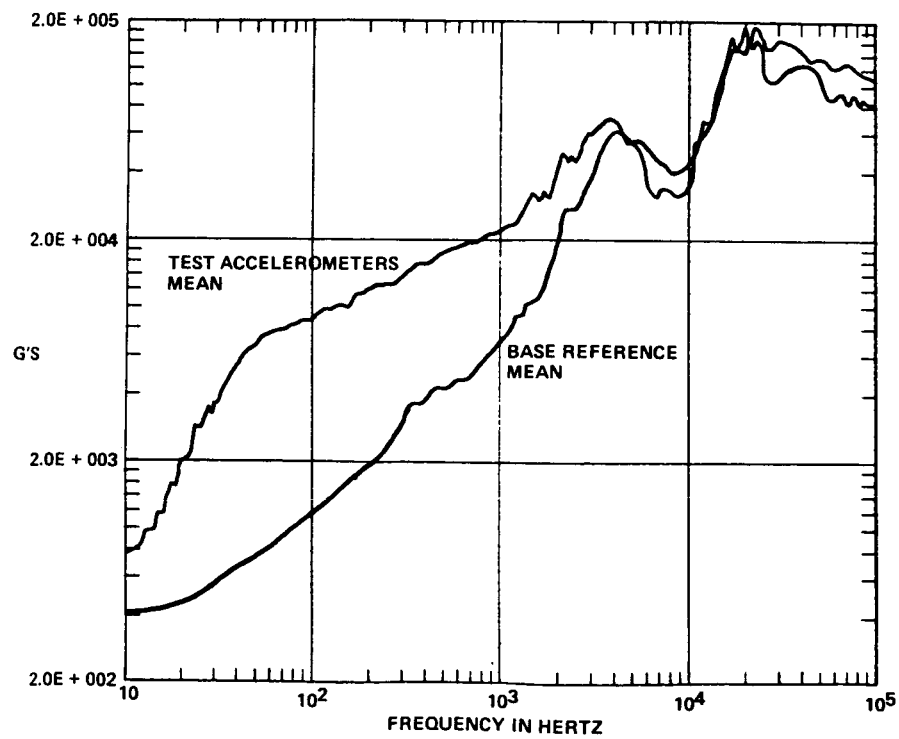

Figure 22. Test accelerometers versus base reference mean.

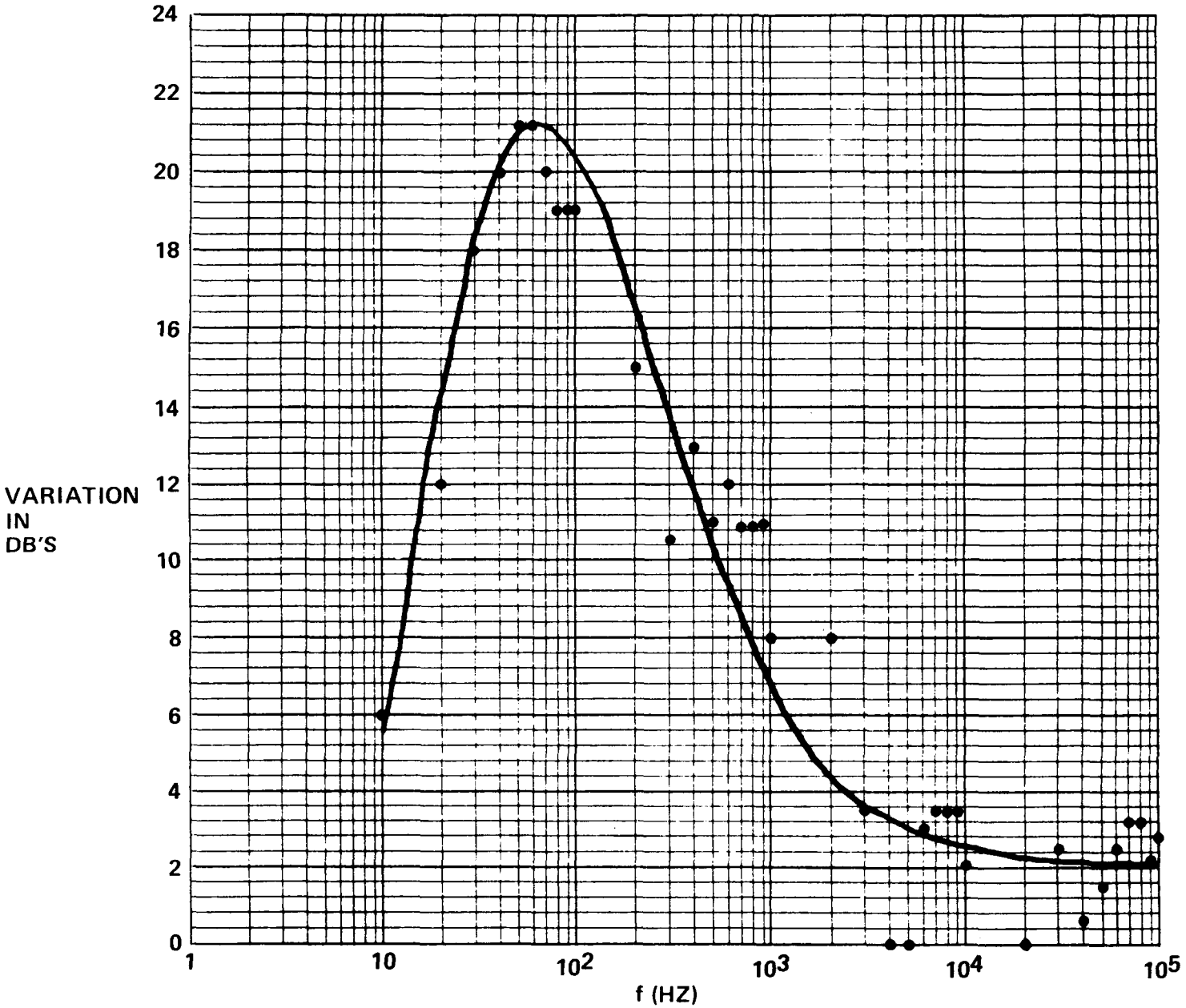

Figure 23. Shock response spectra error due to instrumentation.

Figure 24 illustrates the data envelopes, and Figure 25 illustrates the alloy tests versus unslotted design alloy. Clearly, design alloy and test alloy produce the same SRS. Figurew 26 and 27 illustrate the same results for test alloy versus design alloy for slotted plates. Figures 28 and 29 illustrate envelopes and mean SRS for test alloy versus design alloy for all 10 tests (slotted and unslotted).

Figures 30 and 31 illustrate the envelopes and mean SRS from the five slotted tests versus the mean SRS from the five unslotted tests. Once again, the preliminary analysis is proven. SRS does not vary with target thickness as long as complete severance occurs.

Figure 32 illustrates the predicted SRS at the source and 40 in. from the source. These predictions were based upon the NASA guidelines in the seven volume report, Engelsferd and Radar [3]. One remarkable result from the variables tests (section c) shows that shock level does not vary with distance from the two source for this particular test (explained in next section). The "at source" prediction corresponds exactly to our data up to about 1100 Hz. Considering the development of instrumentation from 1970 to 1985 and the fact that mounting blocks were used, it is evident that these prediction techniques were state-of-the-art at that time. Recall the 7270 envelope of the first 10 shots (Fig. 21). Figure 33 is the mean SRS derived for shots 1 through 10. This mean was used for comparisons in the variability section of the paper. The straight lines illustrate the theoretical slopes of 6 dB/octave up to approximately 10,000 Hz and 0 dB/octave above 10,000 Hz. Compare Figures 32 and 33. The instrumentation in 1970 was not sufficient to analyze the upper frequency (above 10,000 Hz) of pyroshock systems. Also, most instrumentation in 1985 is not capable of high frequency measurement either. Instrumentation completely accounts for upper frequency discrepancies.

C. Variability

The purpose of the variability portion of the plate tests was to evaluate manufacturing and assembly parameters as well as some supplementary tests. The three most obvious variables were coreload, standoff, and coupling (the amount of torque on the screws in the FSA). Each one of these was investigated individually and in combination.

Two shots were performed for maximum coreload and for minimum coreload. Tolerances for 30.0 grain/ft LSC are ±2.3 grains/ft deliberately used 35 grains/ft and 27 grains/ft LSC (these sections of LSC had been rejected by quality personnel in manufacturing because they exceeded tolerance limits) to over emphasize this parameter. Figure 34 is an envelope of SRS data for maximum and minimum coreload. Notice that very little spread exists between upper and lower envelope bounds for both envelopes. Figure 35 is an SRS plot for the maximum coreload mean, the minimum coreload mean, and the base reference mean. The very slight differences are well within the instrumentation error band or range. Coreload tolerances do not affect the FSA SRS.

Recommended standoff for 30 grain/ft RDX aluminum LSC cutting aluminum is 0.191 in. with tolerances being 0.221 in. maximum and 0.161 in. minimum. For the test, values of 0.191 in. and 0.221 in. were used. Figures 36 and 37 illustrate the SRS data envelopes and the mean comparisons. Once again, very little variation is noted. Standoff tolerances do not affect FSA SRS.

The FSA coupling torque tolerances are 160 in. lb and 190 in. lb. These values were used for the tests. Figures 38 and 39 are the SRS data envelopes and the maximum, minimum, base reference mean SRS comparisons. Once again, the coupling tolerances do not affect the FSA SRS.

Next, coreload, standoff, and coupling were combined in a combination test series. Originally, the intent was to use the previous single variable test to specify the proper combination. Since little

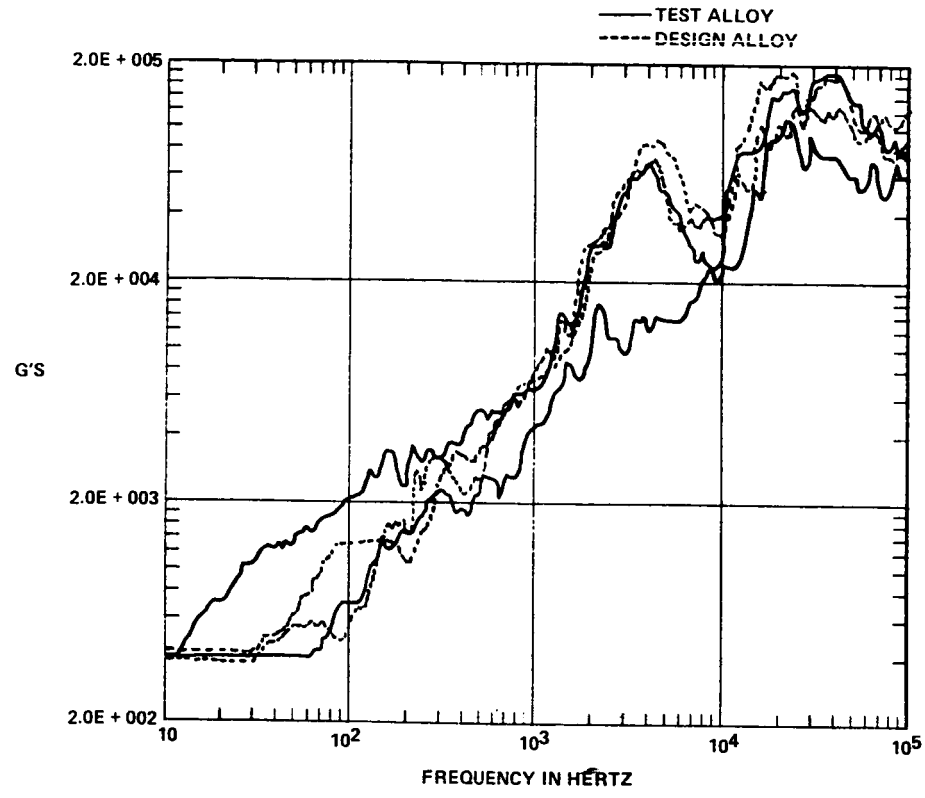

Figure 24. SRS envelopes: test alloy versus design alloy – unslotted plates.

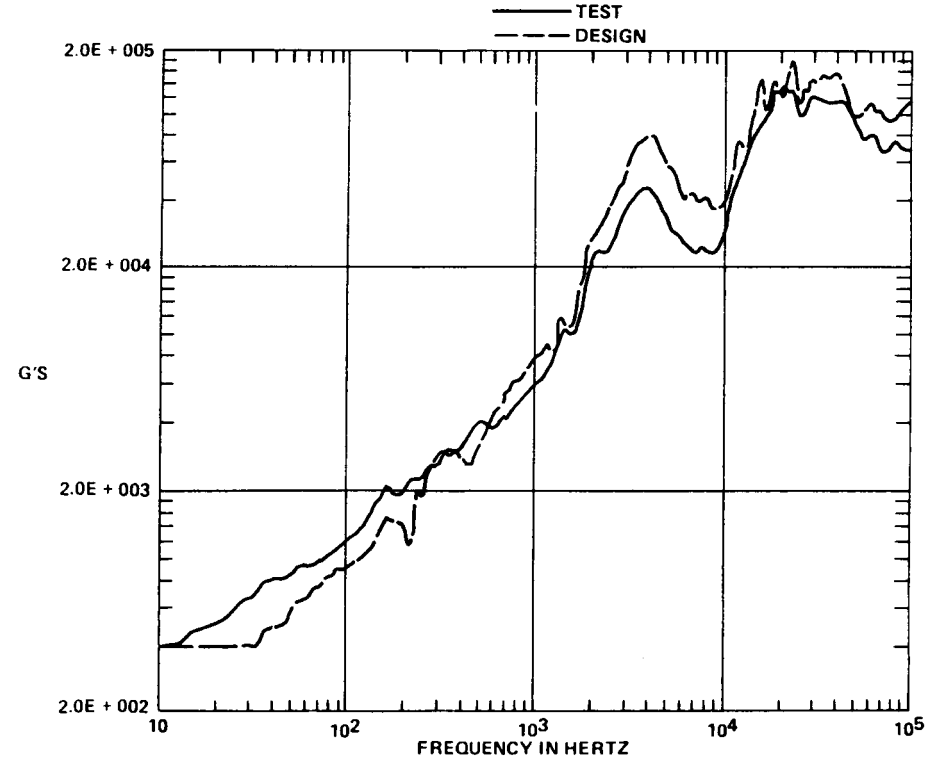

Figure 25. SRS means: test alloy versus design alloy – unslotted plates.

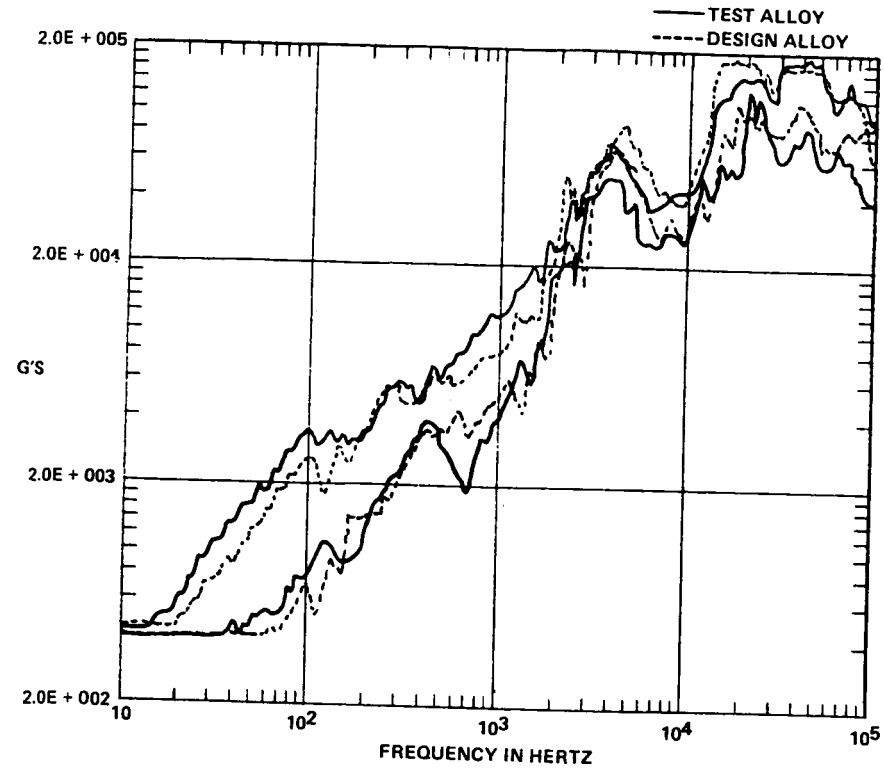

Figure 26. SRS envelopes: test alloy versus design alloy – slotted plates.

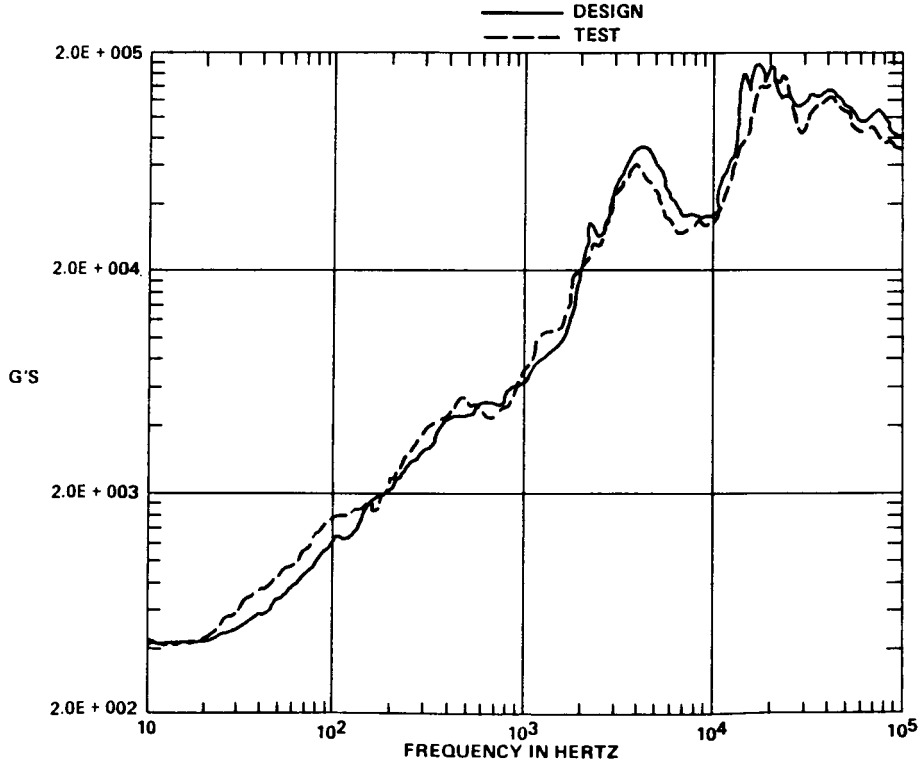

Figure 27. SRS means: test alloy versus design alloy – slotted plates.

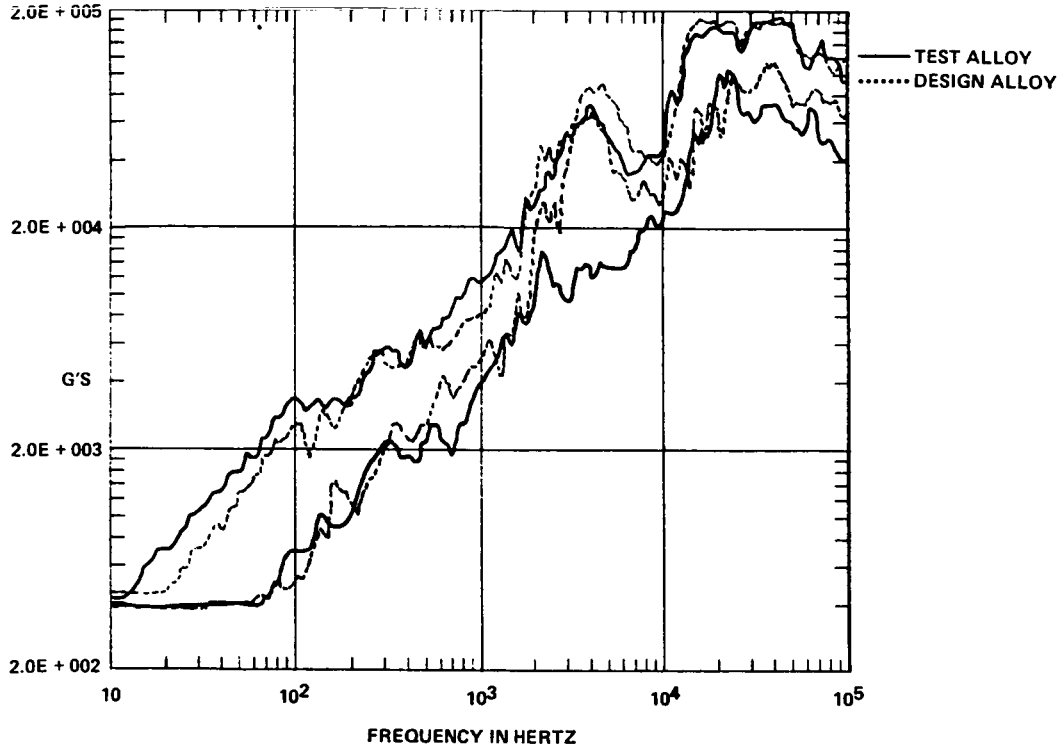

Figure 28. SRS envelopes: test alloy versus design alloy – all ten tests.

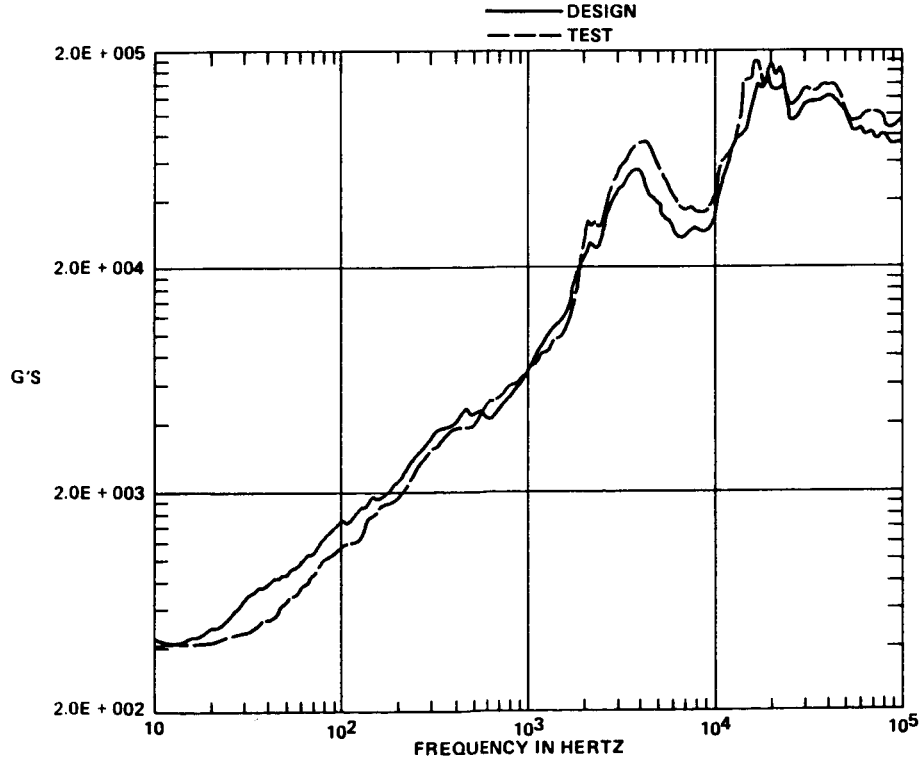

Figure 29. SRS means: test alloy versus design alloy – all ten tests.

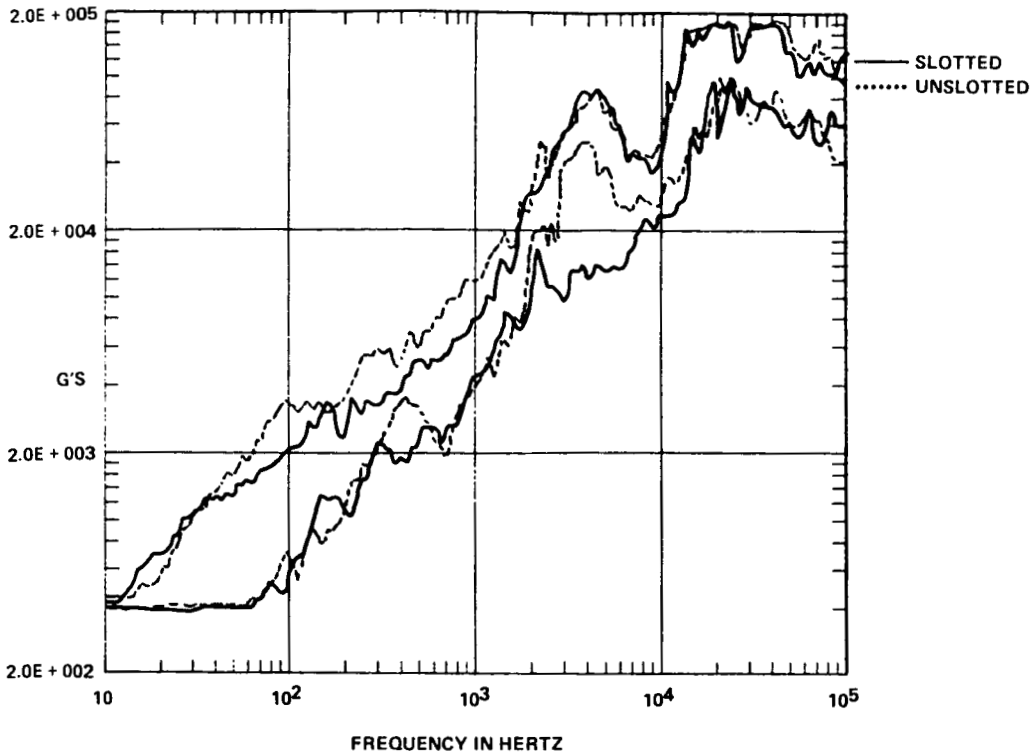

Figure 30. SRS envelopes: slotted versus unslotted – all alloys.

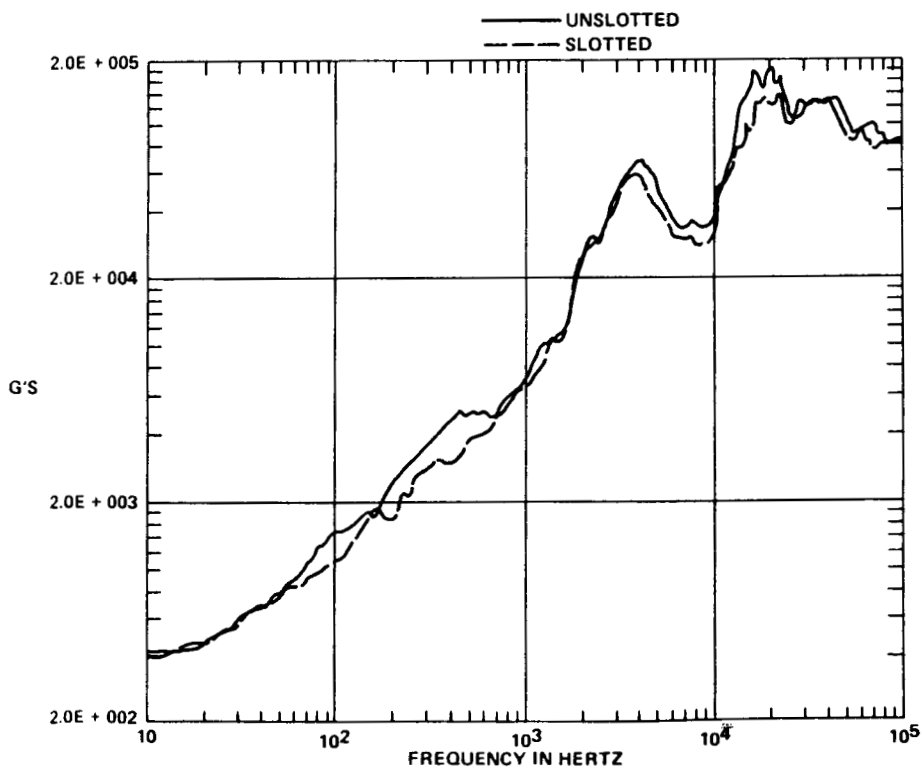

Figure 31. SRS means: slotted versus unslotted – all ten tests.

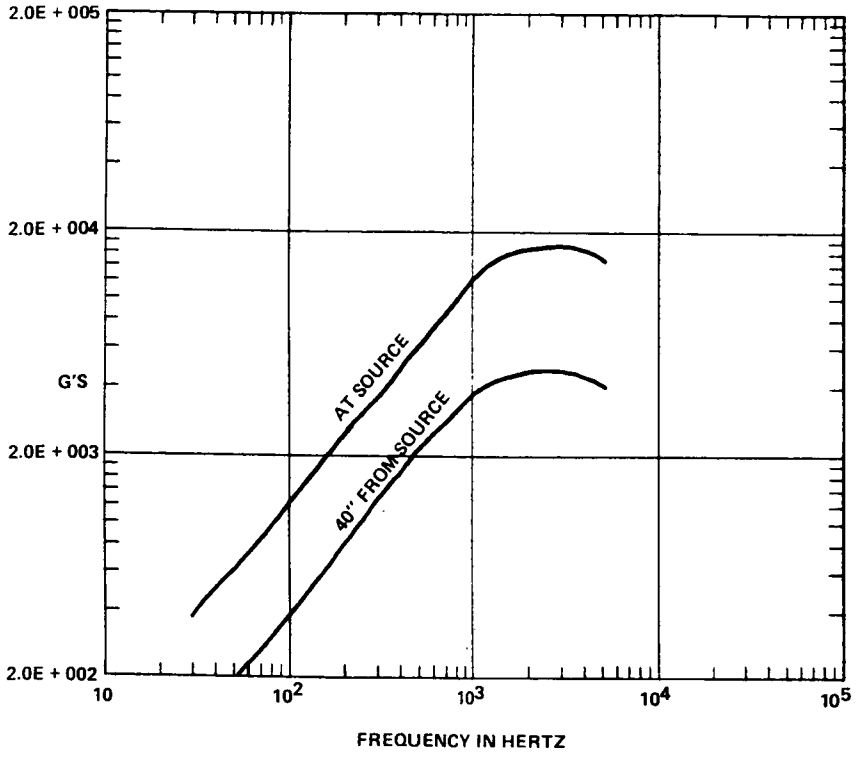

Figure 32. Predicted SRS.

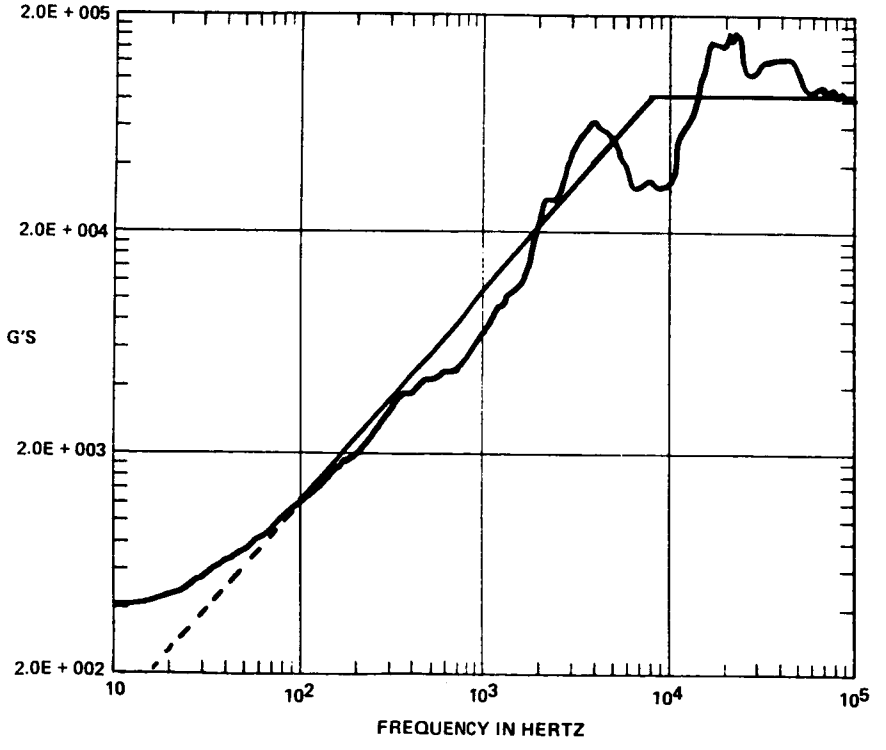

Figure 33. Basic shock response spectra mean.

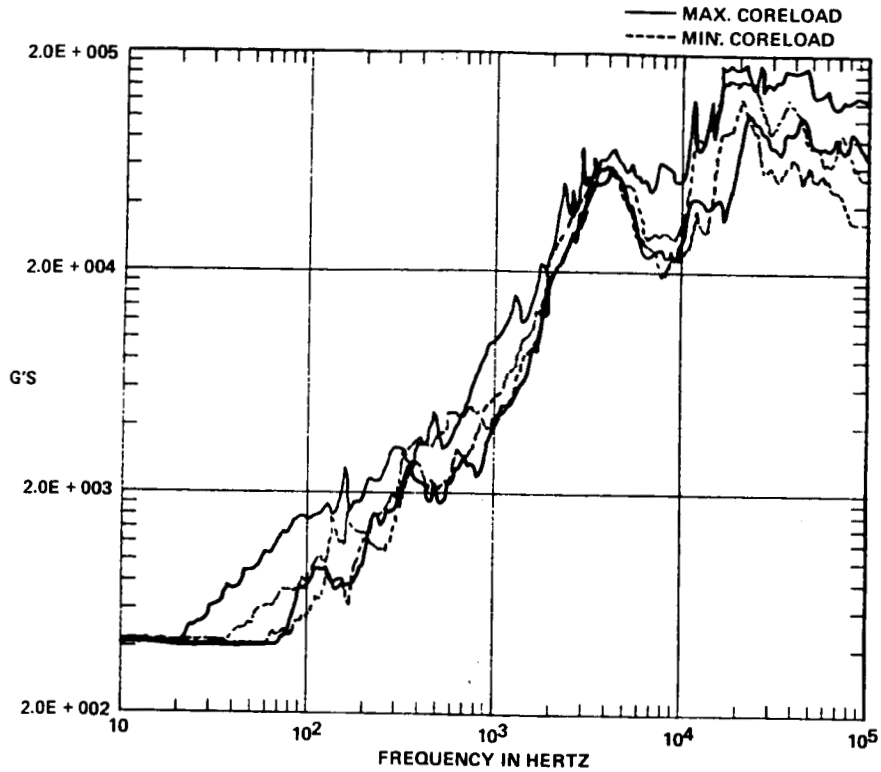

Figure 34. SRS envelope: maximum versus minimum coreload.

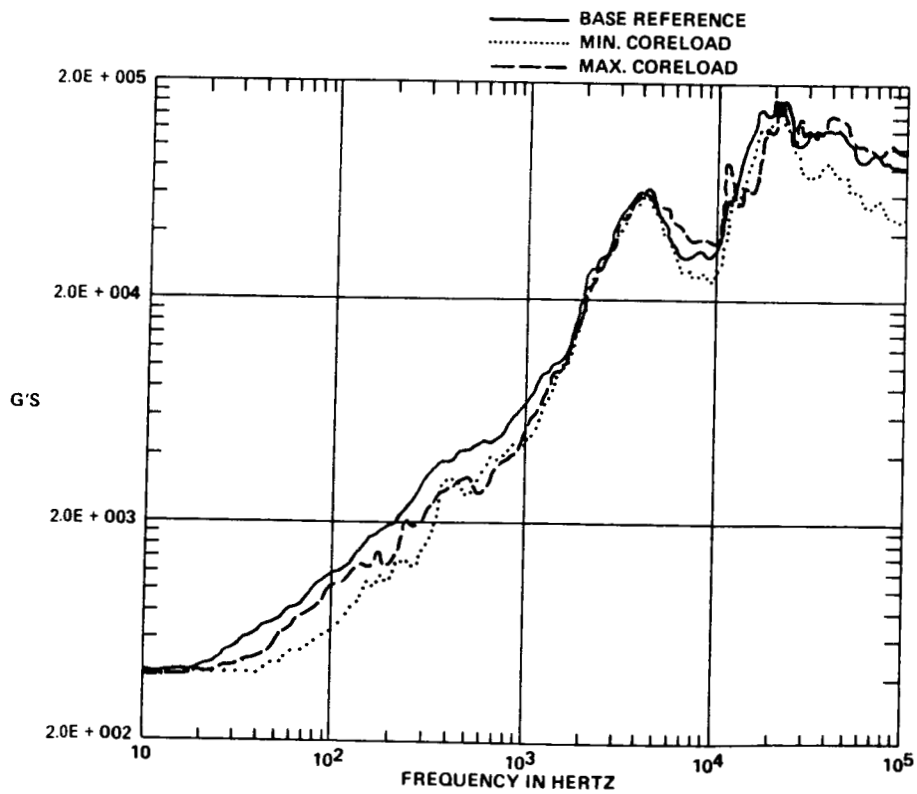

Figure 35. SRS means: maximum versus minimum coreload.

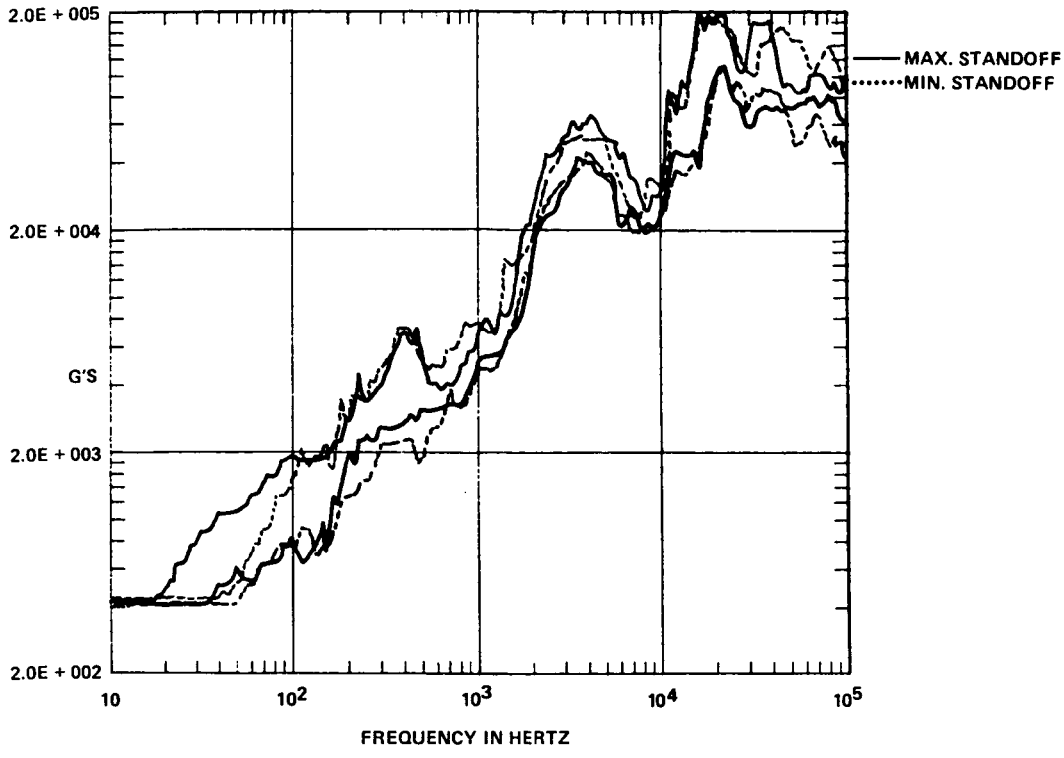

Figure 36. SRS envelope: maximum versus minimum standoff.

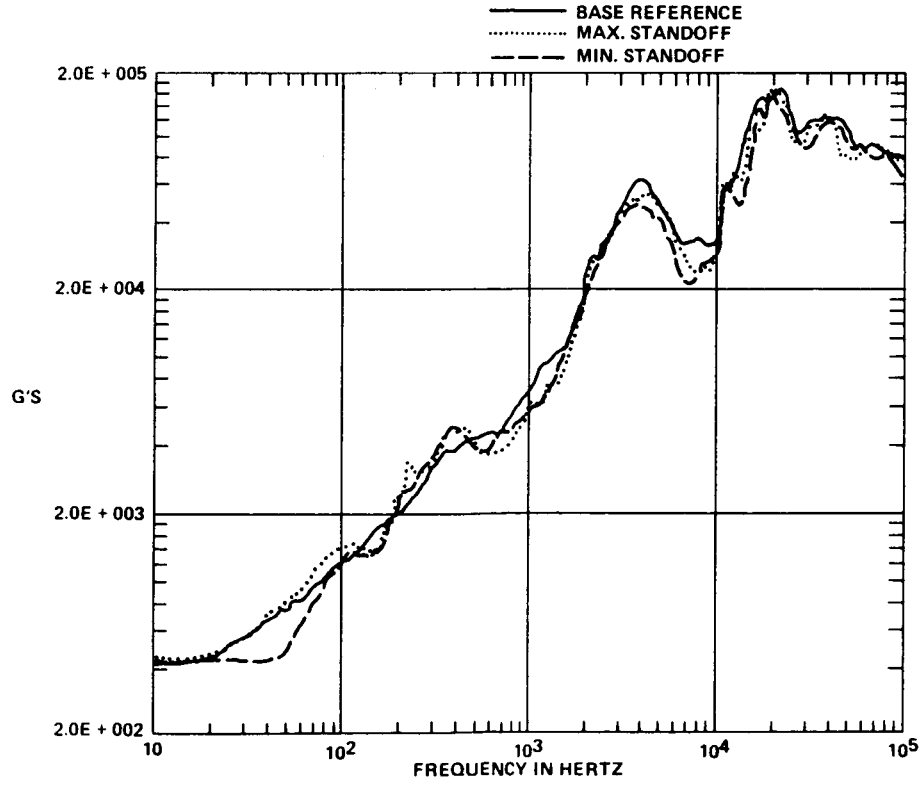

Figure 37. SRS means: maximum versus minimum standoff.

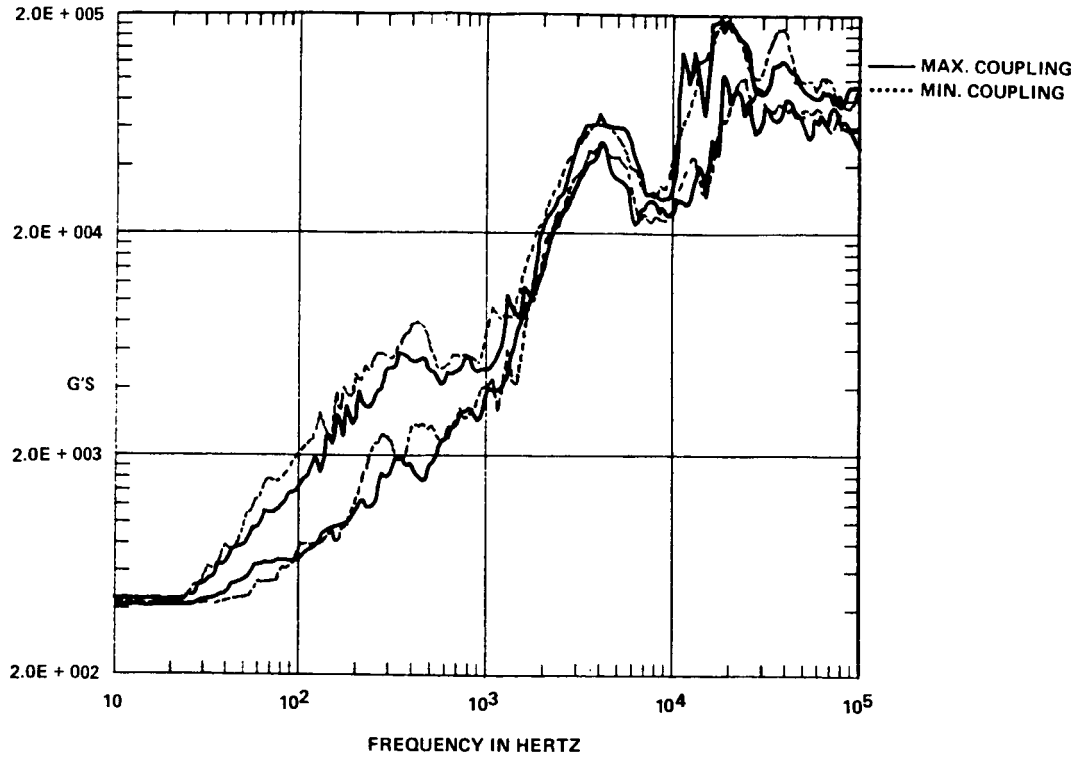

Figure 38. SRS envelopes: maximum versus minimum coupling.

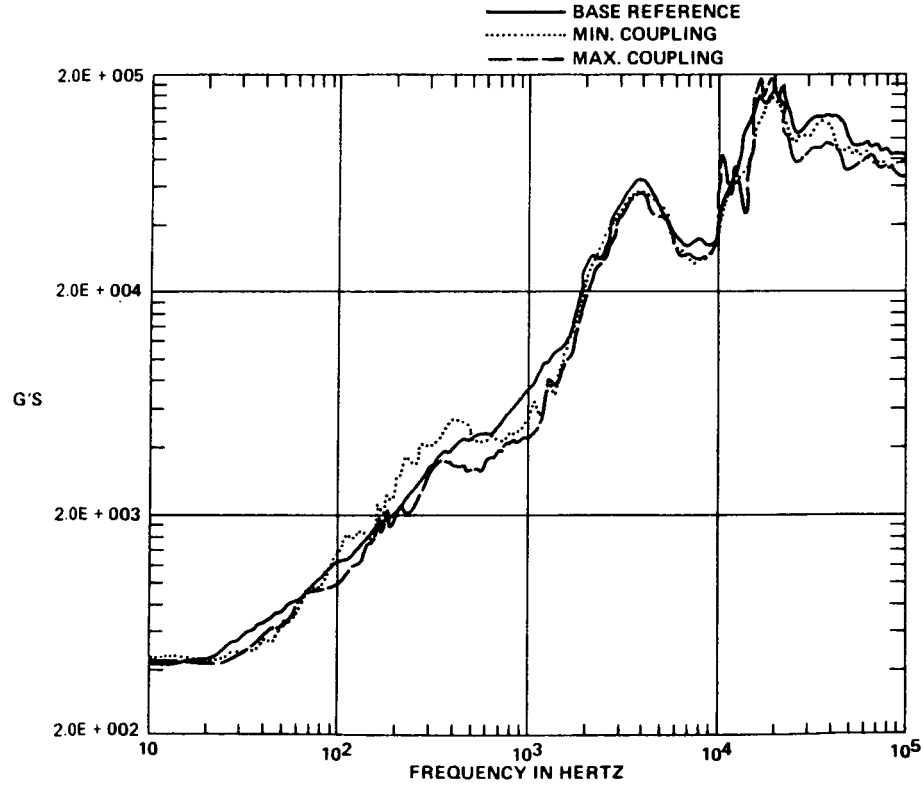

Figure 39. SRS means: maximum versus minimum coupling.

or no variation occurred singlely, the combinations were specified based upon logic. Obviously, one would expect maximum coreload to produce the maximum shock. Likewise, maximum coupling would produce less damping, thus, a higher shock value. Minimum standoff produces a much broader cut with less cutting depth. This should produce a higher shock since more energy would be transferred into the plate. Therefore, the maximum combination was maximum coreload, minimum standoff, and maximum coupling. The minimum combination is minimum coreload, maximum standoff, and minimum coupling. One would expect any variations due to parametric variability to be additive. However, the envelopes (Fig. 40) and the means (Fig. 41) show about the same variation as the individual variables. These findings prove beyond any doubt that coreload, coupling, and standoff tolerances do not significantly affect the FSA SRS.

The next test was a supplementary examination of joint effects. As outlined previously, a 3 in. joint was formed next to the FSA using FSA bolts and torque values. One 7270 accelerometer was placed next to the joint, while the other 7270 remained at the original position away from the source. Figure 42 compares the near source envelope with the away or far source envelope. Figure 43 represents the near source mean, far source mean, and base reference mean SRS. Clearly, a lap joint has little effect upon SRS. However, there does appear to be slight changes in the ultra-high frequency (approaching 100 Hz) region, as expected. These variations could be due to instrumentation because the near source data should be higher than the far source data in the ultra-high frequency range. It is clearly evident that very little change takes place in the 30 in. of plate between the two accelerometers. This can be explained because little energy is lost through the bungee restraints and the plate has very little damping.

Another manufacturing variable was investigated in two supplementary plate tests. LSC apex angle tolerances are maximum (98 deg) and minimum (89 deg). Figure 44 illustrates the maximum and minimum apex angle SRS envelopes. Figure 45 contains maximum and minimum apex angle SRS means and the base reference SRS mean. A slight variation is noted between 2000 and 5000 Hz. One would expect the maximum apex angle to produce a greater shock level. However, this variation is small enough that it might also be attributable to instrumentation. Another variation exists between 40 and 200 Hz. Variations below 100 Hz are attributable to noise and the sensitivity of the accelerometers. Overall, these variations are slight. Apex angle tolerances do not affect the FSA SRS.

The next supplementary tests were on the accelerometer mounting method. Most pyroshock test engineers use mounting blocks. These blocks allow the accelerometer to be placed nearer the source; survivability is also increased. But, these blocks are mechanical filters; the "true" shock is not measured. Figure 46 represents the envelopes for 7270 accelerometers, side-by-side, one mounted flat, one on a standard 1-in. cube mounting block. Figure 47 represents the base reference mean SRS, the flat mounted mean SRS, and the block mounted mean SRS. It is clearly evident that the mounting block is a mechanical low pass filter decreasing high-frequency data beginning at 6000 Hz.

A supplemental test without variables was conducted to evaluate triaxial response. It is already accepted that pyroshock response is the same in all three axes. To verify this fact, two plate tests were conducted with three 7270 accelerometers mounted upon a 1-in. mounting block. During the first test, the Y axis channel was lost due to instrumentation. This instrumentation failure (probably within an amplifier) dc shifted the other two accelerometers and all three channels were unusable. The second test saw the same Y axis failure; however, the Z axis (perpendicular to the plate) and the X axis (parallel to the short axis of the plate) were good data. Figure 48 shows the base reference mean and the X and Z axes actual data (not mean). No envelopes were included since test No. 33 failed. Some variation in the X and Z data is attributable to the Y axis failure. For all practical purposes, the X and Y axes are the same. Notice that both axes are below the base reference above 2000 Hz due to the mounting block.

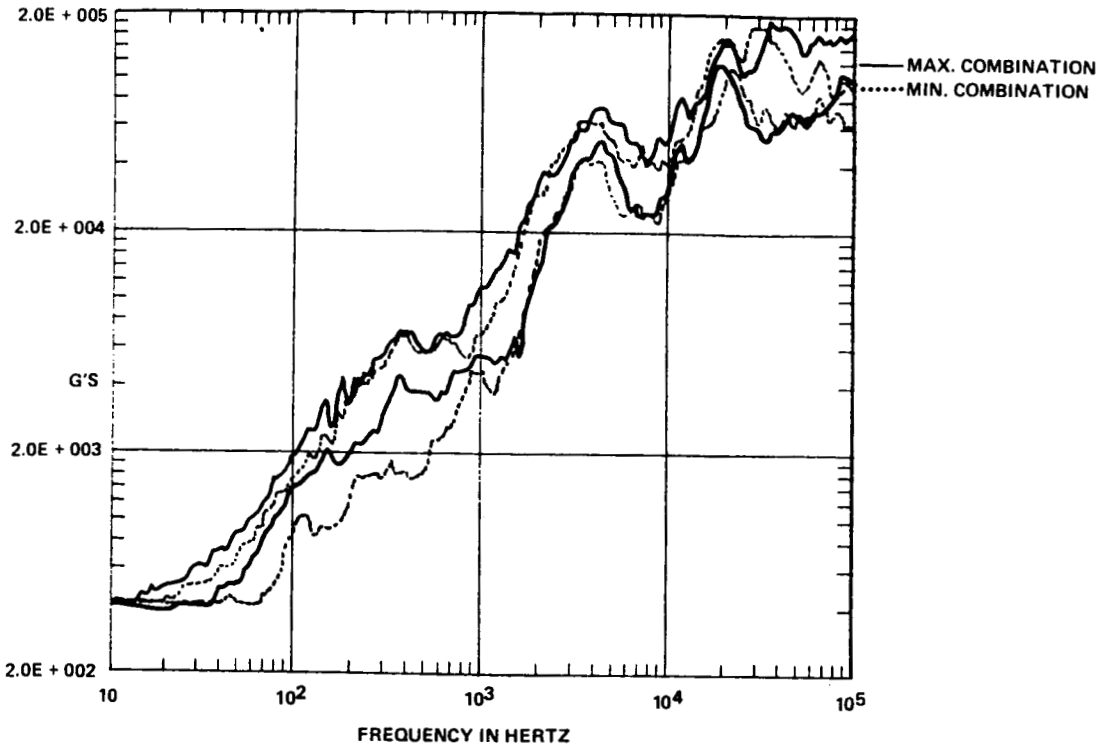

Figure 40. SRS envelopes: maximum versus minimum combination.

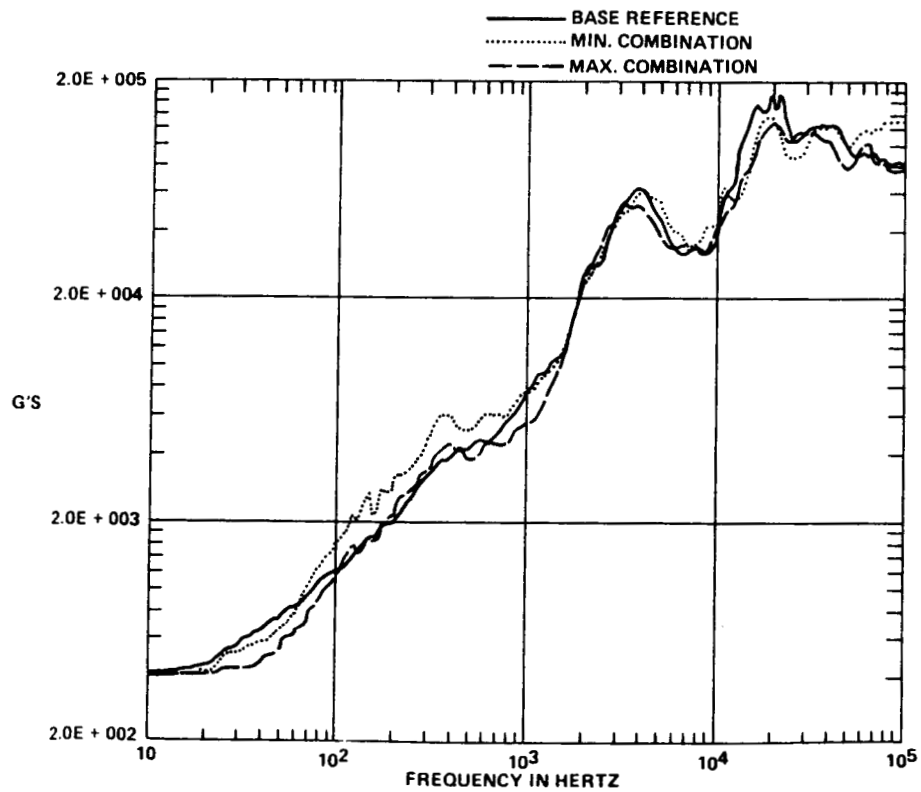

Figure 41. SRS means: maximum versus minimum combination.

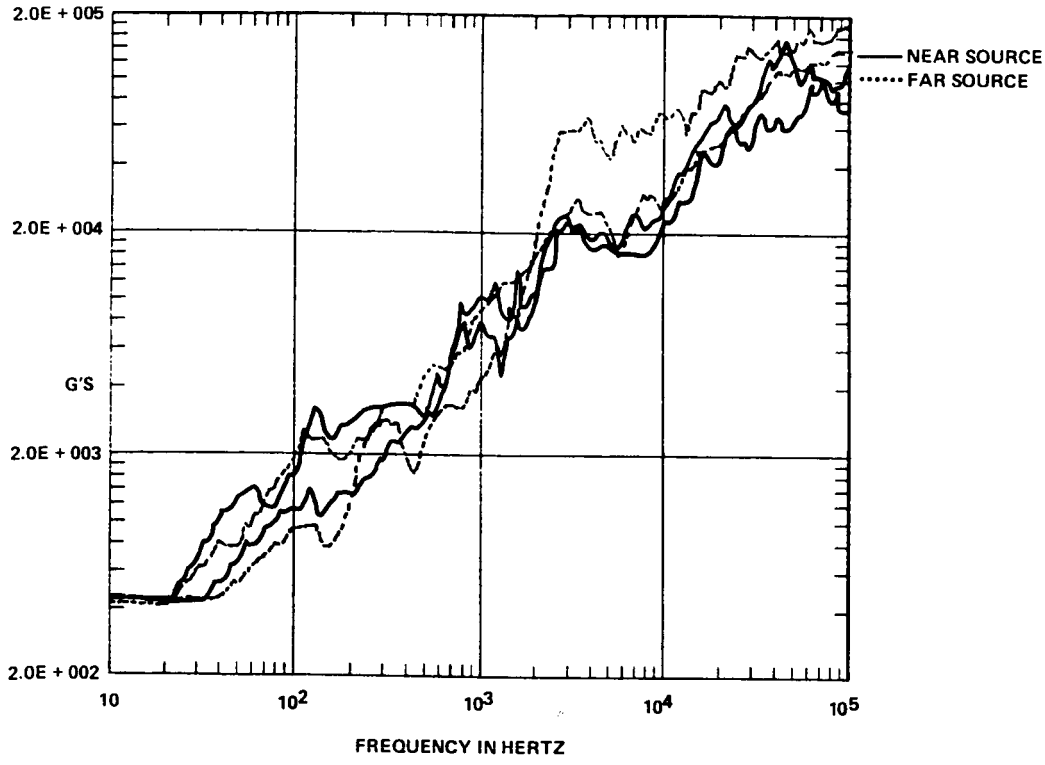

Figure 42. SRS envelopes: joint tests: near versus far source.

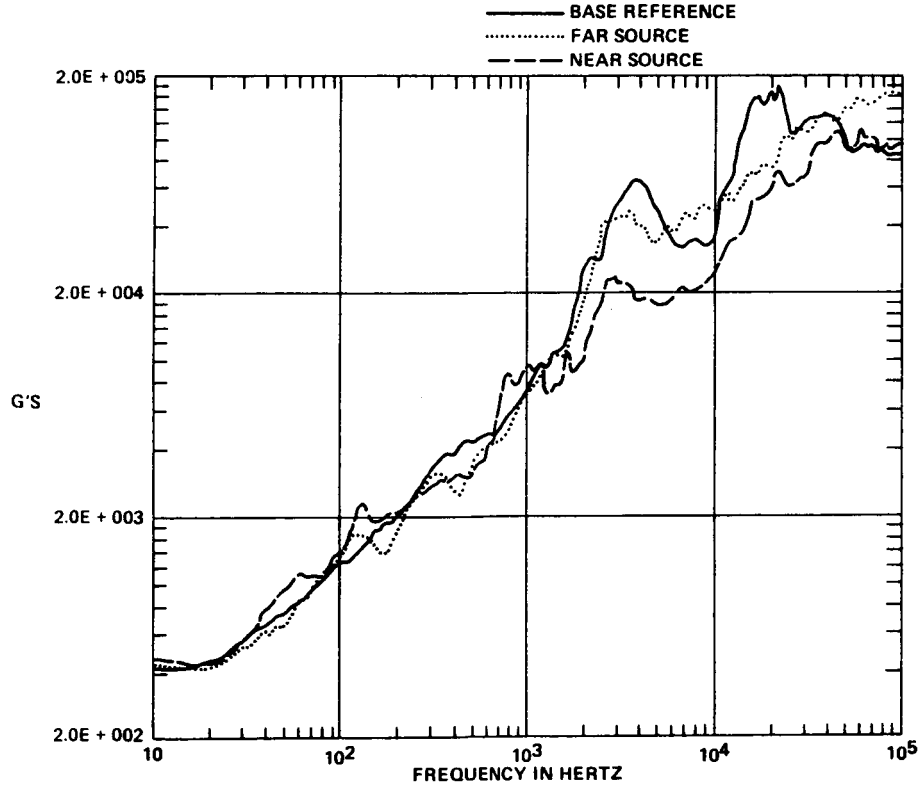

Figure 43. SRS means: joint tests: near versus far source.

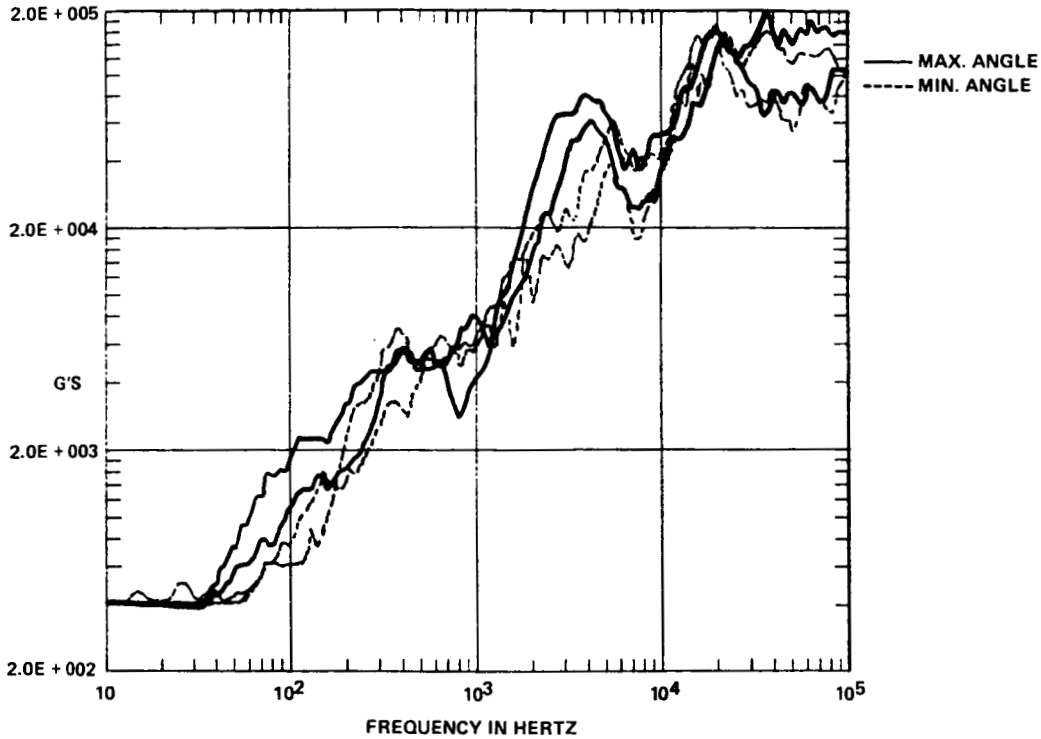

Figure 44. SRS envelopes: maximum versus minimum apex angle.

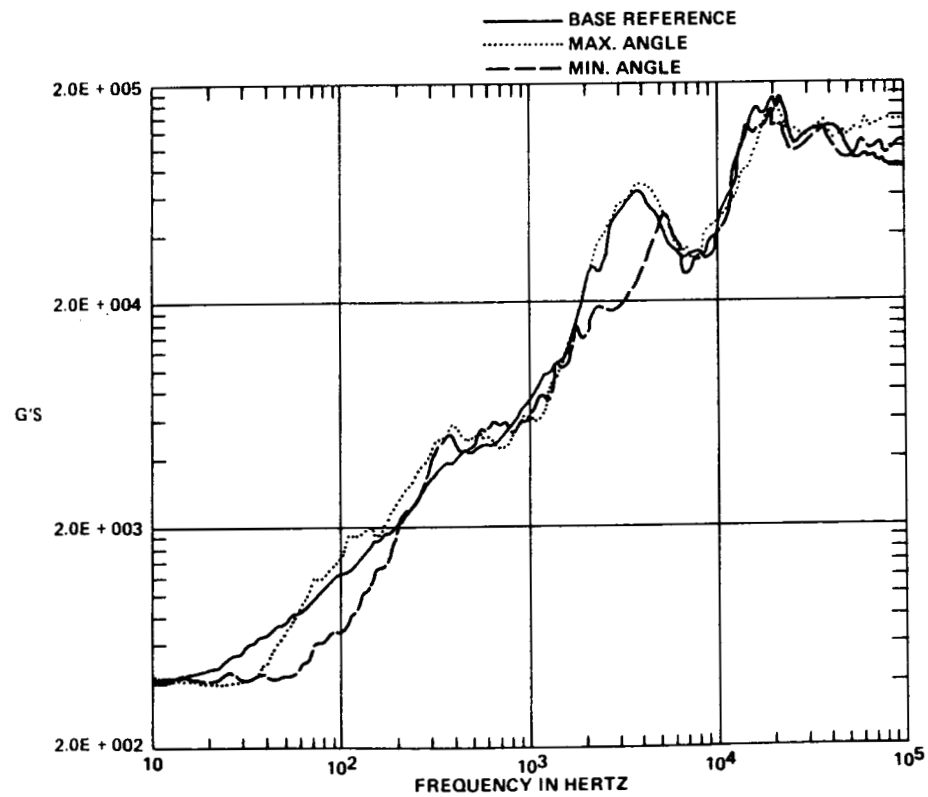

Figure 45. SRS means: maximum versus minimum apex angle.

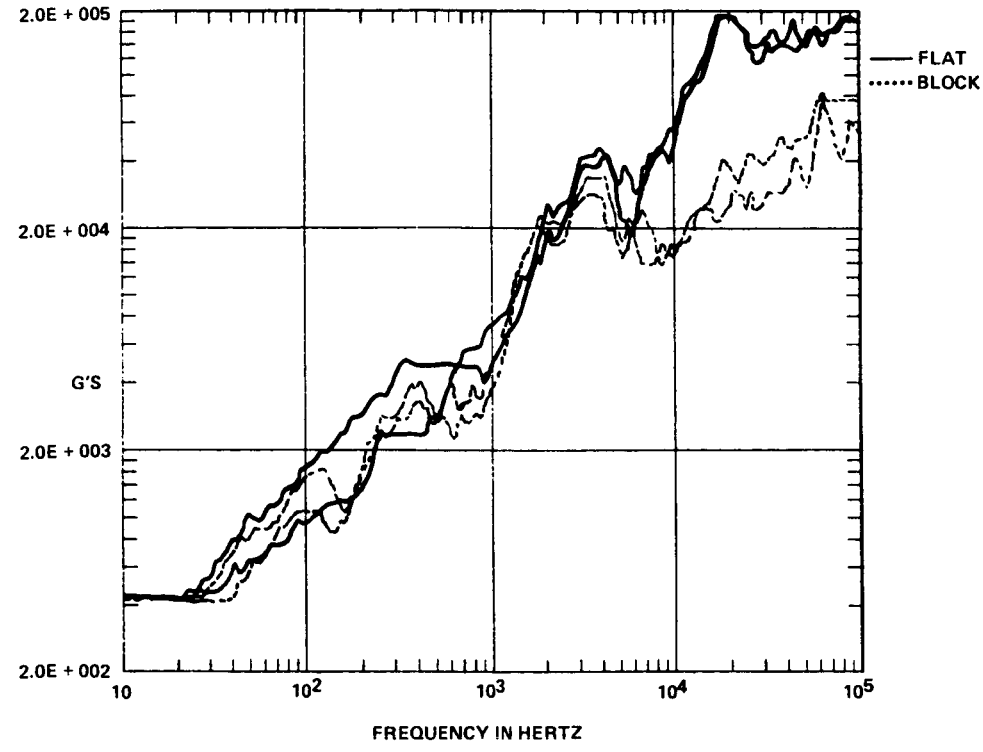

Figure 46. SRS envelope: accelerometer mounting: flat versus block.

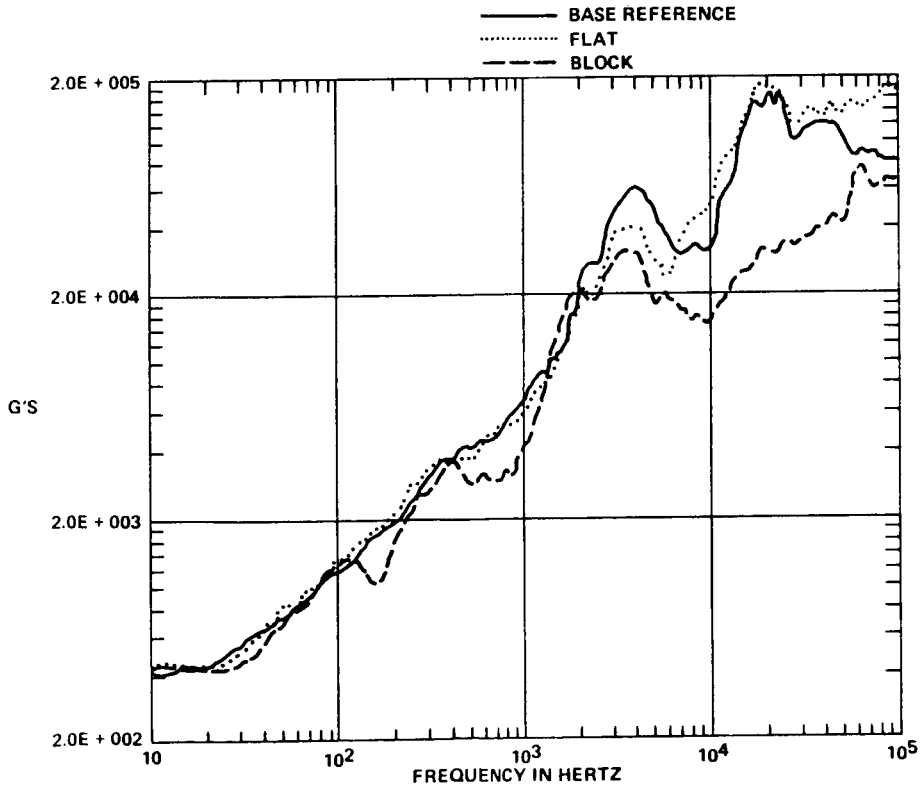

Figure 47. SRS means: accelerometer mounting: flat versus block.

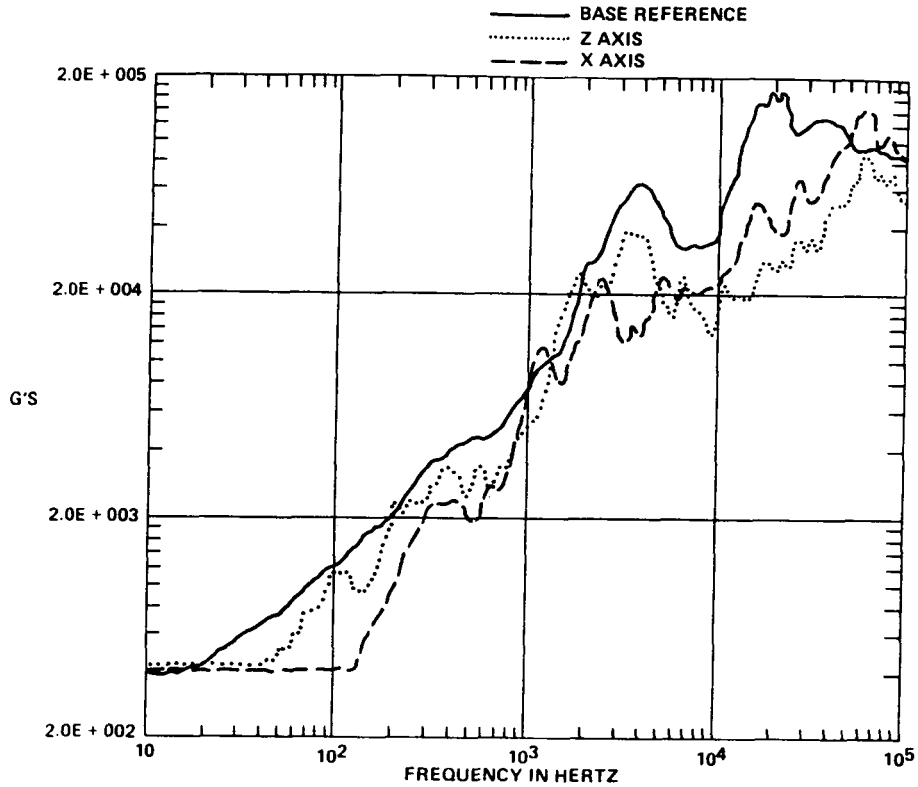

Figure 48. SRS multi: axis comparisons.

The final supplemental test involved gross coreload variation. Coreloads of 40 and 25 grains/ft were used. Figures 49 and 50 illustrate the low and high gross coreload envelopes and the mean comparisons. No variation is noted between the shocks produced by the 25 and 40 grains/ft charges. It is evident that if the plate is severed completely the shock is about the same regardless of coreload.

Additional analysis using Fourier transform plates indicates the same results as the shock response spectra. The Fourier plots were most useful in locating accelerometer resonances.

D. Data Correction Techniques

Specialized data correction techniques for pyroshock are not yet available because appropriate software has not been developed to manipulate time history data. Data correction was not needed for the 7270 data because of the high degree of accuracy of the data measured by it. Further analysis of the test accelerometer or non-7270 data is warranted at a future date utilizing the methods outlined by Smith [63]. The following is an example of data correction methodology.

Figure 51 is a time history plot from one of the preliminary tests recorded by a 7270 accelerometer. Figure 52 is time history recorded by an Endevco 2255A-005 accelerometer 1 in. from the 7270 on the same shot. Figure 53 illustrates the uncorrected displacement time history for the acceleration time history in Figure 52. Notice that the final displacement is 100 ft. Figure 54 is a linearly corrected displacement time history of the plot in Figure 53. Notice the final displacement is 0.6 ft with the maximum displacement only about 1 ft. Figure 55 represents the corrected acceleration time history. Figure 56 contains SRS from the 7270 and from the 2255A-005 before and after correction. Notice that the error is in the low frequency range; above 3000 Hz no error exists. There is still an error for the

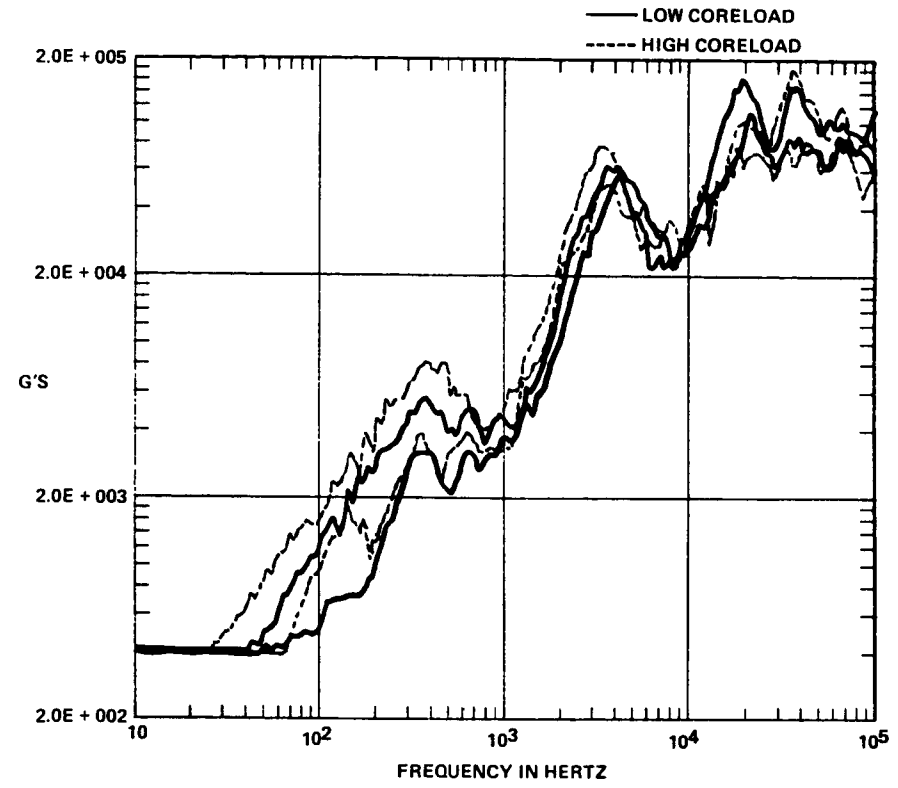

Figure 49. SRS envelopes: low versus high gross coreload.

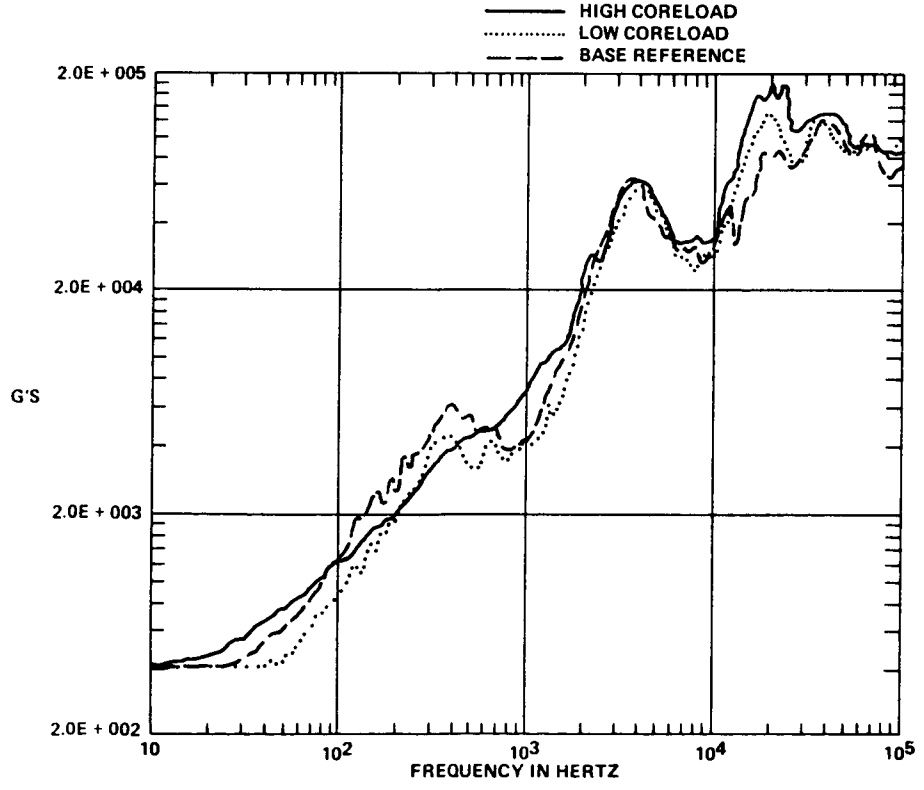

Figure 50. SRS means: low versus high gross coreload.

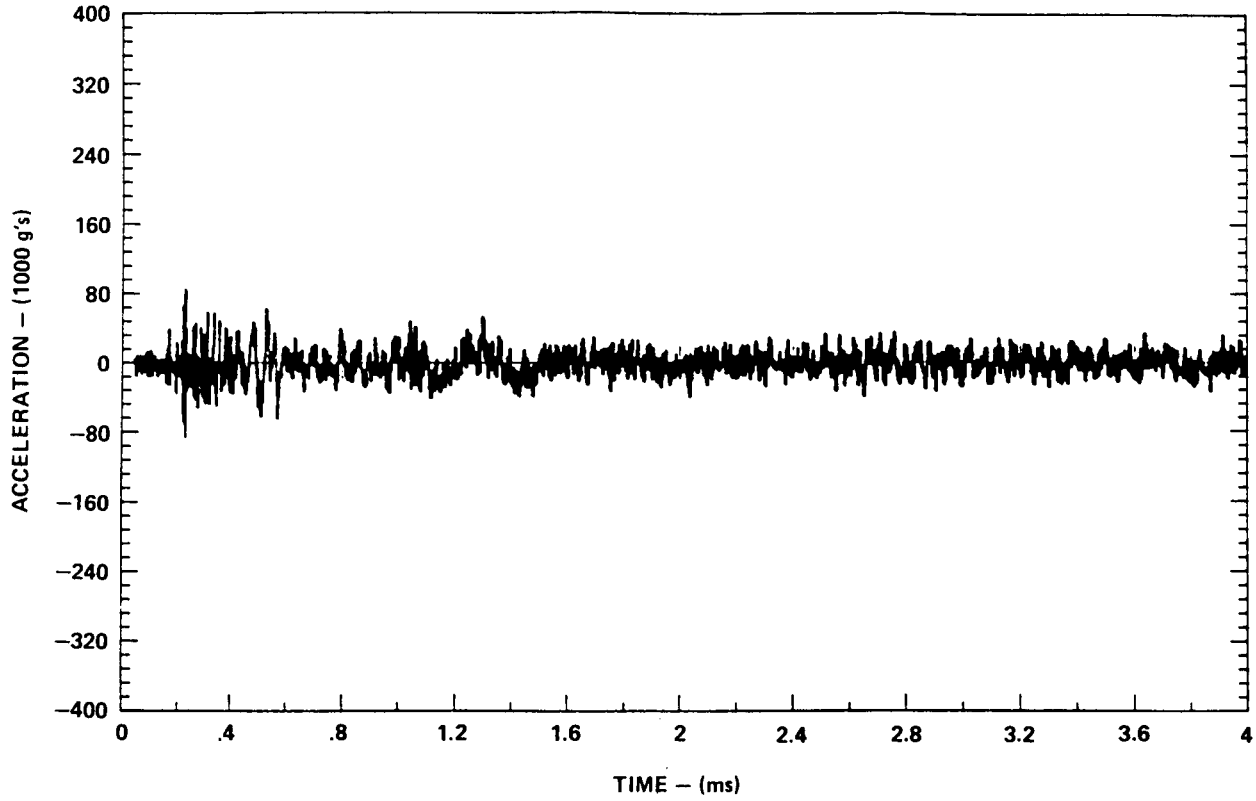

Figure 51. Acceleration time history – 7270.

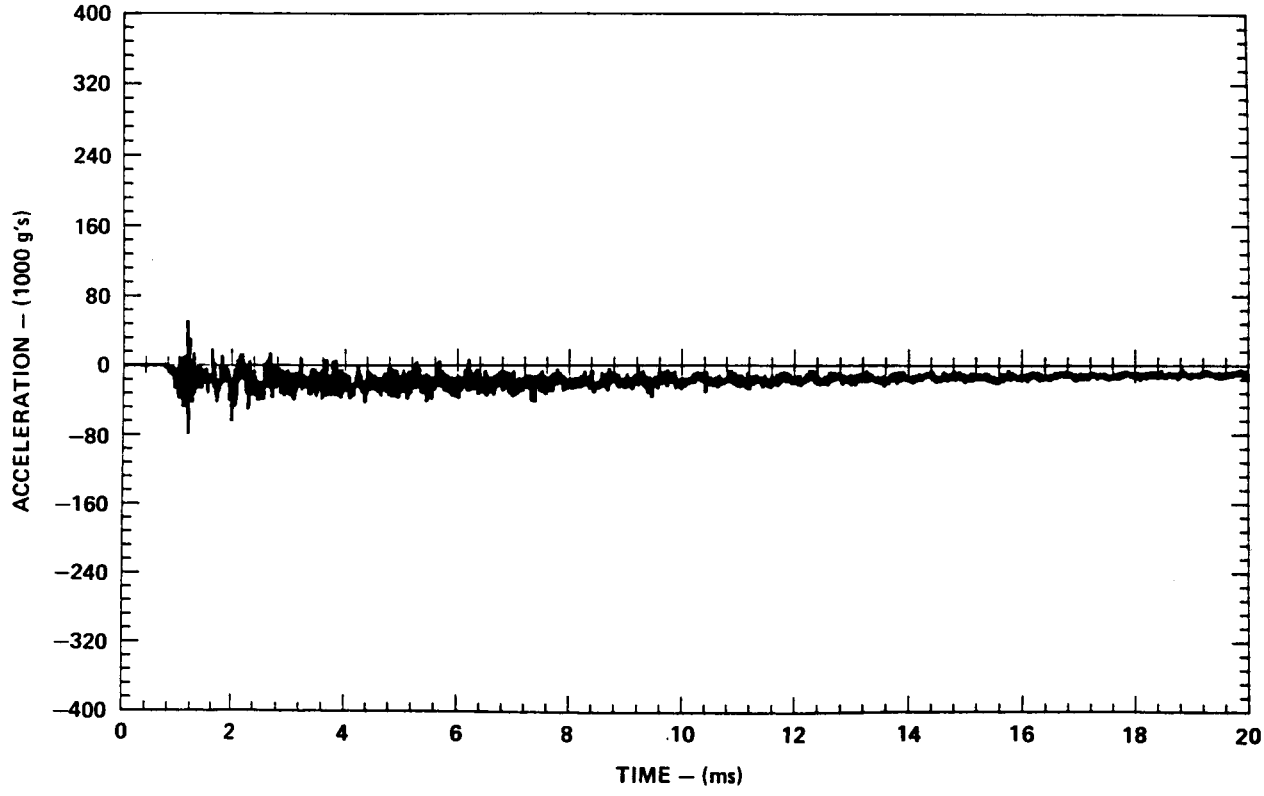

Figure 52. Acceleration time history – baseline shifted.

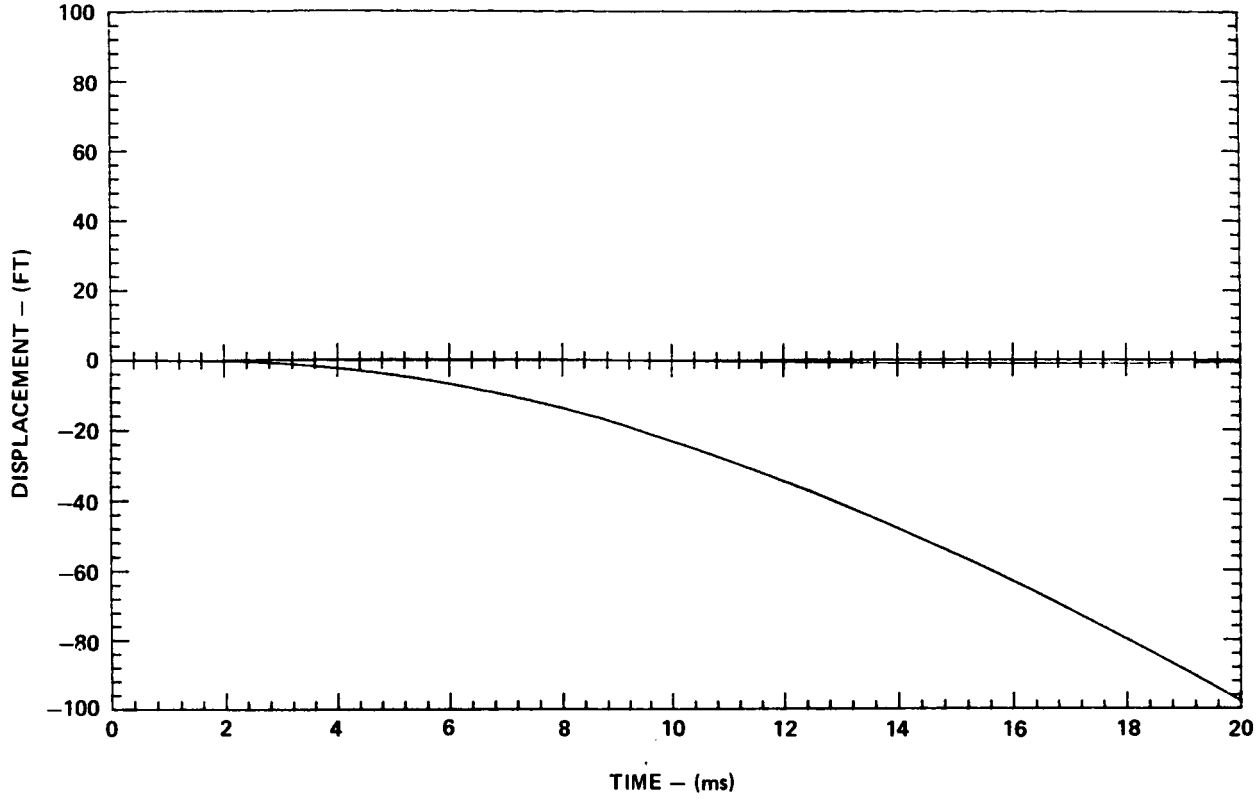

Figure 53. Uncorrected displacement time history.

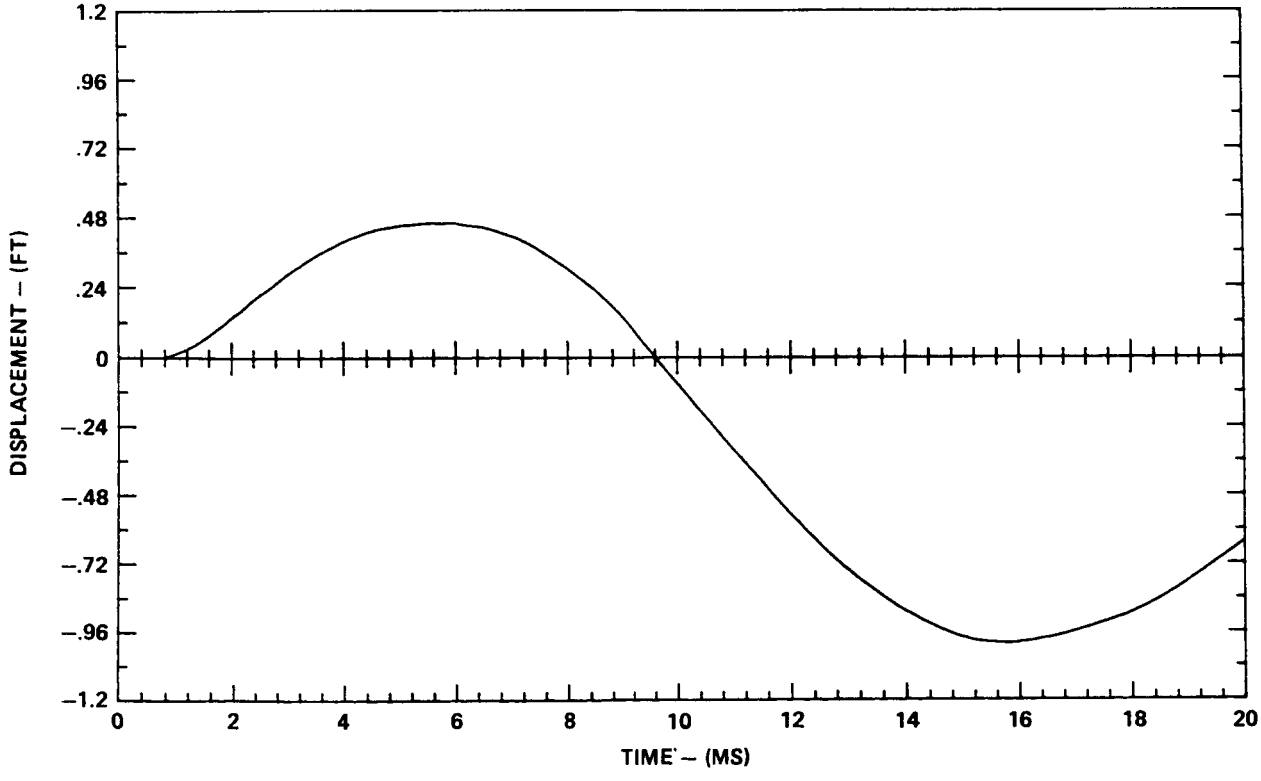

Figure 54. Linearly corrected displacement time history.

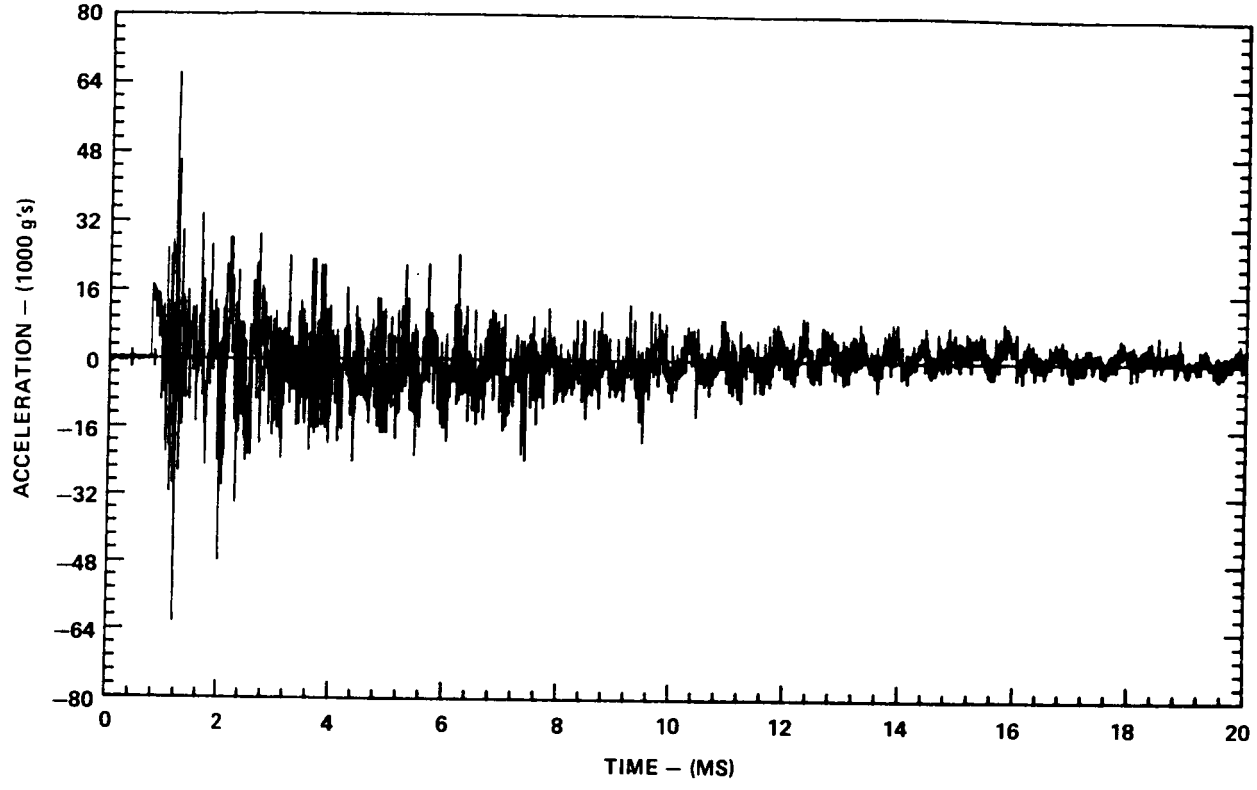

Figure 55. Linearly corrected acceleration time history.

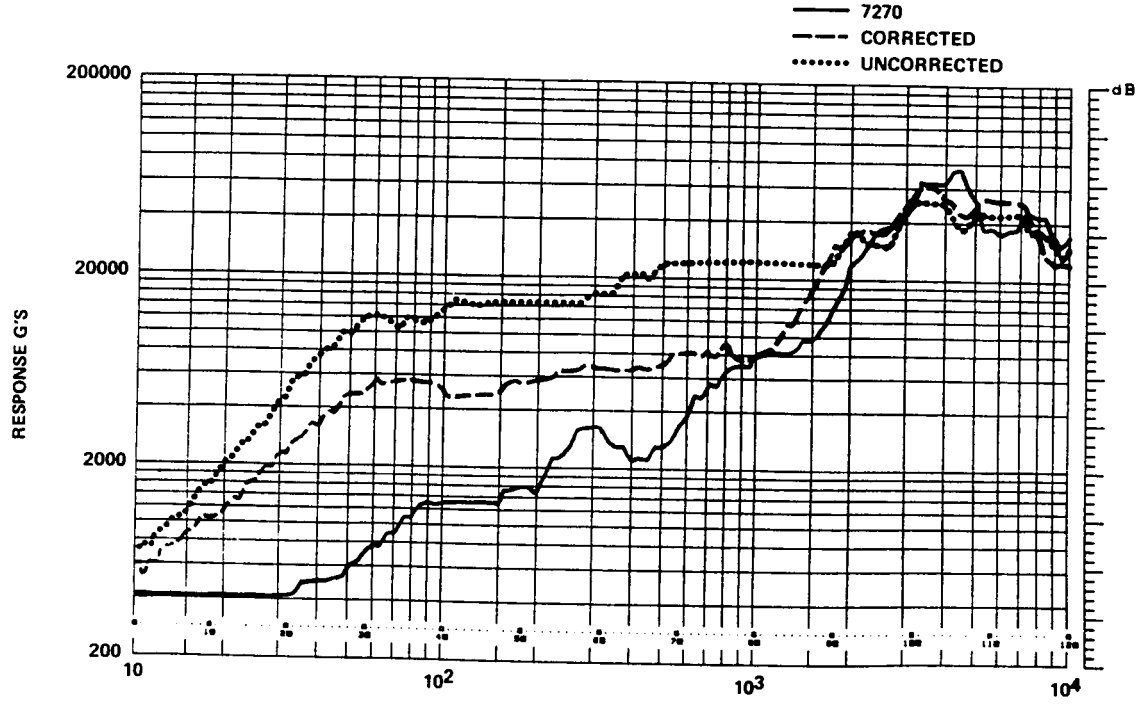

Figure 56. SRS-7270 versus uncorrected versus corrected data.

corrected data. These corrections were done by hand by trial and error just to demonstrate that the theory of correction is good. Once a computer algorithm is designed, correction methodology will be much quicker and much more accurate. A curved correction of these data was needed instead of a linear correction. This accounts for the small "hump" still remaining in the SRS.

VI. SUMMARY, CONCLUSIONS, AND RECOMMENDATIONS

A. Summary

The loss of two Solid Rocket Boosters in 1982 prompted NASA to investigate why variations of 50 percent (6 dB) or more were measured for the same location from pyrotechnic test to pyrotechnic test. These variations, reported throughout the industry, raised many questions regarding shock response spectra repeatability from similar explosive sources, and the precision and accuracy of the shock data.

A major research effort was organized to analyze variations in pyrotechnically induced shock response spectra and to determine if and to what degree manufacturing and assembly tolerances, distance from the charge, data acquisition instrumentation, and shock energy propagation affect the shock response spectrum.

The test program was divided into three areas: precision and accuracy, basic shock response spectra, and variability. Precision and accuracy consisted of ball drop calibration testing of the test accelerometers and 28 preliminary plate tests. The results of the plate tests were used to direct the flow of the remaining test program. Data from the entire test program were used to evaluate instrumentation in this area. The Endevco 7270 accelerometer was the only accelerometer giving good results. Accelerometer error as a function of frequency was documented. The 7270 also demonstrated the highest level of survivability.

Basic shock response spectra consisted of ten plate tests used as a control case. The only variables involved were aluminum alloy variety and plate thickness (target area thickness). Analysis indicated that alloy variety would not affect the shock response spectra. Also, analysis indicated that target thickness would not affect the shock response spectra as long as complete plate severance occurs. The 7270 accelerometer data were very repeatable. Other accelerometers were used side-by-side with the 7270's for instrumentation evaluation. Most non-7270 data were baseline shifted and erratic. A base reference mean shock response spectra was derived from the ten tests. This spectra was used in variability for a control case comparison.

Variability consisted of 26 plate tests used to evaluate manufacturing and assembly variables and supplemental variables. Variables consisted of coreload, standoff, coupling, LSC apex angle, and gross variation of coreload. These were evaluated by test individually. Data indicated none of these affected the shock response spectra. Combination tests of coreload, standoff, and coupling yielded the same results. Two joint tests were performed (lap joint – 3-in. overlap) and indicated that the ultra-high frequency decreased very slightly. Two accelerometer mounting tests (flat versus block mounted) indicated a significant decrease in high frequency occurs when mounting blocks are used. The final supplementary tests indicated that the plate response to pyroshock is about the same for all axes. The final result is that shock response spectra do not vary with manufacturing and assembly tolerances and instrumentation is the one major problem associated with pyroshock measurement.

B. Conclusions

Several conclusions may be drawn from this study. Clearly, unlike popular belief, shock response spectra from the same source are very repeatable when proper instrumentation is used. The 50 percent (6 dB) or more variations encountered in most previous studies were probably due to instrumentation. New accelerometer designs should eliminate many of the large variations. Surprisingly, shock levels are much higher overall, especially in the high frequency range above 10,000 Hz. These high frequency, high acceleration levels are very capable of destroying electrical and electronic components, especially accelerometers. Baseline shifts and accelerometer resonances have distorted most pyroshock data in the past. Only the new Endevco 7270 accelerometer gave "good" data during this study. All other accelerometers gave distorted data or failed altogether. One can conclude that instrumentation is just on the verge of being able to accurately measure pyroshock.

Variations in coreload, standoff, charge holder coupling, and LSC apex angle do not affect shock response spectra as long as complete severance occurs. Manufacturing and assembly tolerances do not affect shock response spectra. Also, the shock response spectra is the same for all three axes when the shock is generated by linear-shaped charges.

Lap joints do not affect the shock response spectra below 10,000 Hz. A slight decrease is noted above 10,000 Hz. Accelerometer mounting methodology is very important. Most past studies used mounting blocks. Mounting blocks act as mechanical filters removing high frequency data. Therefore, the "true" shock is not measured. One can conclude from flat mounted accelerometer data that mounting blocks should not be used in pyrotechnic tests, because they remove high frequency data that are sufficient to destroy flight hardware.

One may also conclude that the 1970 NASA study and the seven volume report are accurate for low frequency data (less than 1000 Hz).

Data analysis indicates that shock level is not a function of distance from the source for this test fixture. However, one should be careful to note that for this test fixture free-free plate conditions existed and total energy is not dissipated very rapidly as a function of distance. If the long sides of the plate, perpendicular to the charge axis, had been clamped, the energy levels would have dissipated rapidly with distance.

C. Recommendations

The author advises NASA to investigate possible instrumentation errors in their flight failure. Future test series need to be conducted to investigate joint effects upon shock response spectra, all types of joints should be included. Test series need to be conducted with accelerometers starting at the source and continuing outward in 1-in. increments to investigate shock response spectra as a function of distance from the source for non-free-free conditions. Tests need to be performed where incomplete plate severance occurs.

The author also advises all test personnel to refrain from using mounting blocks in pyroshock testing.

Further study is especially warranted, since the new accelerometer, the Endevco 7270, is able to accurately record shock data near the source without accelerometer resonance or baseline shifting.

Tests need to be performed upon real space structures to determine energy changes for various structures.

REFERENCES

1. Hieber and Tustin: Understanding the Shock Response Spectrum. Sound and Vibration, 1974, pp. 42-54.

2. Kacena, W. J., McGrath, M. B., and Rader: Aerospace Systems Pyrotechnic Shock Data-Ground Test and Flight. Volumes 1 through 6, Martin Marietta Corporation, 1970.

3. Engelsferd, I. K., and Rader, W. P.: Aerospace Systems Pyrotechnic Shock Data/Ground Test and Flight. Volume 7, Martin Marietta, 1970.

4. Clark, N. H.: How Accurate is Your Accelerometer. Vibration and Noise Control Eng., Sydney, Australia, 1976, pp. 105-106.

5. DeVorst, V. F. and Hughes, P. S.: Piezoelectric Accelerometer Signal Error in Complex Shock Recordings. U. S. Naval Ordnance Laboratory, Paper NOLT67-194, 1967.

6. Keller, Leo A., Jr.: Linear Vibration Techniques for Measuring the Cross Axis Error Coefficient in an Accelerometer. AIAA Paper, No. 80-1763, New York, 1980, pp. 297-308.

7. Sawyer, G.: Transducer Reliability – Who is to Blame? Noise and Vibration Control Worldwide, Vol. 13, No. 3, 1982, pp. 118-120.

8. Harris, Cyril M. and Crede, Charles E.: Shock and Vibration Handbook. Second Edition, McGraw-Hill Book Co., 1976, pp. 1-23.

9. Thomson, William T.: Theory of Vibration with Applications. Prentice-Hall, Inc., Englewood, New Jersey, 1981.

10. Luhrs, H. N.: Pyrotechnic Shock Testing – Past and Future. IES: Proceedings of Annual Technology Meeting, 1981, pp. 17-20.

11. Bai, M., and Thatcher, W.: High G Pyrotechnic Shock Simulation Using Metal-to-Metal Impact. SVB, No. 49, Part 1, 1979, pp. 97-100.

12. Bell, R. L.: Development of 100,000 G Test Facility. SVB, Vol. 40, Part 2, 1969, pp. 205-214.

13. Conway, J. J., Pugh, D. A., and Sereno, T. J.: Pyrotechnic Shock Simulation. Proc. IES, 1976, pp. 12-16.

14. Conway, J. J. and Sereno, T. J.: Pyrotechnic Shock Testing of Components. Proc. IES, 1977, pp. 109-112.

15. Luhrs, H. N.: Pyrotechnic Shock Transmission in Component Versus S/C Testing-Vibration Table Compared with Instrumented Spacecraft Model. Proc. IES, 1975, pp. 3-27 to 3-44.

16. Fandrich, R. T., Jr.: Bounded Impact – A Repeatable Method for Pyrotechnic Shock Simulation. SVB, No. 46, Part 2, 1976, pp. 101-107.

17. Fandrich, R. T., Jr.: Pyrotechnic Shock Testing on a Standard Drop Machine. Proceeds of IES 20th Annual Meeting, 1974, pp. 269-273.

18. Davie, Neil: Personal interview. Sandia National Laboratories, 1985.

19. Sill, Robert: Personel Interview. Endevco Corporation, 1985.

20. Sill, R. D.: Testing Techniques Involved with the Development of High Shock Acceleration Sensors. Endevco Corp., San Juan Capistrano, CA, 1983.

21. Nilsson, L. and Nilsson, B.: Method for Testing Components in the High Acceleration Frequency Range. Luleaa University, Tulea-1981-18, 1981.

22. Keegan, W. B. and Bangs, W. F.: Effects of Various Parameters on Spacecraft Separation Shock. SVB, No. 42, Part 3, 1972, pp. 131-148.

23. Lieberman, P.: Pyrotechnic Plate Analysis and Test Results of Missile and Space Vehicle Hardware. Internal Instrumentation Symposium, 25th, 1982.

24. Liebermann, P.: Pyrotechnic Simulation Techniques to Test Missile and Space Vehicle Hardware. IES No. 84-45551 22-14, 1983, pp. 153-158.

25. Powers, D. R.: Development of a Pyrotechnic Shock Test Facility. SVB, No. 44, Part 3, 1974, pp. 73-82.

26. Schoessow, T. D.: Deviation of Shock Environmental Criteria-Characteristics of Barrel Tester for Shock Test Environment Generation. Proceedings of Aerospace Testing Seminar – Conference on Reliability Engineering and Quality Control Testing of Aerospace Vehicle Components, Sunnyvale, CA.

27. Kyuma, Kazuo, Shuichi Tai, and Masahiro Nunoshita: Fiber-Optic Sensing Systems. Central Research Lab., Denshi, Tokyo, No. 21, 1982, pp. 98-101.

28. Hicho, M. D.: Logical Engineering Approach to Vibration Transducer Selection. Noise and Vibration Control Worldwide, Vol. 13, No. 3, 1982, pp. 109-113.

29. Pilcher, James O., II: Acceleration Measurements in High G Environments. U.S. Army Ballistic Research Lab., Technical Report BRL-TR-2610, 1984.

30. Lauer, R.: Accelerometers Using Piezoelectric Ceramic Sensors. Electronic Applications Bulletin, Vol. 35, No. 2, 1978, pp. 105-116.

31. Bouche, R. R.: Accelerometers for Shock and Vibration Measurements. ASME AMD, Vol. 12, 1975, pp. 25-59.

32. Kulkarni, V. P. and Ramakrishna, Rao K.: Design and Development of Piezoelectric Accelerometers. Journal of Industrial Engineering (India), Vol. 55, Pt. ET1, 1974, pp. 1-5.

33. Orlacchio, Anthony W.: Shock and Vibration Transducers. Electronic Design, Vol. 22, No. 21, 1974, pp. 68-75.

34. Schelby, F.: Systems Approach to Measuring Short Duration Acceleration Transients. Sandia National Labs., Report SAND-82-1730, 1983.

35. Schelby, F.: Systems Approach to Measuring Short Duration Acceleration Transients. Sandia National Labs., Report SAND-82-1730C, 1983.

36. Schelby, Frederick: Personal Interview. Sandia National Laboratories, 1985.

37. Ball, R. and Lewis, C. P.: Effect of Noise When Driving Signals from Accelerometers. Measurement and Control, Vol. 15, No. 2, 1982, pp. 59-61.

38. Purdy, D.: Vibration Measurements – An Introduction to Piezoelectric Accelerometers and Associated Instrumentation. Noise Control and Vibration Isolation, Vol. 10, No. 5, 1979, pp. 178-181.

39. Marples, V. and Graham, N. A.: Dependence of Piezoelectric Accelerometer Response on Method of Attachments. Journal of the Society of Environmental Engineers, No. 56, 1973, pp. 19-20.

40. Mondshein, Lee F.: Observability of Accelerometer Test-Input Errors. AIAA Paper, No. 80-1762, 1980, pp. 290-296.

41. Brown, G. W. and Drago, G. A.: Shock Calibration of Accelerometers Using Hopkinson's Bar. University of California at Berkeley, 1977.

42. Walston, William H. and Federman, Charles: Fourier Transform Techniques for the Calibration of Shock Accelerometers. National Bureau of Standards, NTIS PB-258982, 1975.

43. Brown, G. W.: High G. Calibration of Accelerometers. University of California at Berkeley, 1975.

44. Bouche, R. R.: High Frequency Shaker for Accurate Accelerometer Calibrations. Journal of Environmental Sciences, Vol. 13, No. 3, 1970, pp. 10-15.

45. Bouche, R. R.: Calibration of Shock and Vibration Measuring Transducers. Bouche Labs., Tujunga, CA, undated.

46. Cannon, J. E. and Rimbey, D. H.: Transient Method of Calibrating a Piezoelectric Accelerometer for the High G Level Range. ASME, Paper 71-Vibr-43, 1971.

47. Clark, N. H.: Developments in Absolute Calibration of Accelerometers at the National Standards Laboratory. Monash University, Department of Mechanical Engineering, Clayton, Victoria, Australia, 1974.

48. Ecker, W.: New Calibration Method for Accelerometers with Wide Ranges. Messtechnik, Vol. 81, No. 12, 1973, pp. 385-393.

49. Ecker, W.: New Procedure for Calibrating High Range Accelerometers. NTIS, UCRL-TRANS-10906/XPS, 1973.

50. Floor, R. Z.: Field Calibration of Accelerometers. International Congress on Acoustics, 6th, Tokyo, Japan- Reports, Vol. 4, 1968, pp. 77-80.

51. Godt, P. W. and Pyle, H. S.: Application of a Laser Interferometer System for Calibrating Accelerometers and Dynamic Pressure Transducers. Journal of Environmental Sciences, Vol. 13, No. 5, 1970, pp. 9-12.

52. Gregory, H.: An Absolute Method of Piezoelectric Accelerometer Calibration. A.Q.D. Labs., Harefield, England, NTIS No. AD729705, 1970.

53. Licht, Torben R. and Yaveri, K.: Calibration and Standards: Vibration and Shock Measurement. Bruel and Kjaer Technical Review, No. 4, 1981, pp. 16-27.

54. Licht, Torben R. and Yaveri, K.: Calibration and Standards: Vibration and Shock Measurement. Measurement and Control, Vol. 15, No. 1, 1982, pp. 9-13.

55. Macinante, J. A.: Recent Developments in Accelerometer Calibration. Monash University, Department of Mechanical Engineering, Clayton, Victoria, Australia, 1974, pp. 381-392.

56. Ramboz, John D.: Comparison and Absolute Calibration of Shock Accelerometers. Proceedings of Shock Symposium and Workshop, Howard Community College, Columbia, MD, 1973.

57. Webster, H. L.: Precision Shock Accelerometer Calibrator. Sandia National Labs., Report CONF-760513-3, 1976.

58. Wittkowski, Ulrich: Shock Pendulum Method for Calibrating and Testing Accelerometers. Tech. Mess TM, Vol. 46, No. 9, 1979, pp. 323-328.

59. Yu, Zhong-Min, Li, Wen-Long, and Dong, Xian-Quan: Absolute Calibration of Accelerometers at High Frequencies. Strain, Vol. 17, No. 1, 1981, pp. 26-27.

60. Luhrs, H. N.: Equipment Sensitivity to Pyrotechnic Shock. Proc. IES, 1976. pp. 3-4.

61. Albers, L.: Pyrotechnic Shock Measurement and Data Analysis Requirements. Proc. IES, Vol. II, 1975, pp. 11-18.

62. Moore, Donald Baker: Memorandum 4DBM-113, Explosive Technology, Fairfield, CA, 1984.

63. Smith, James Lee: Recovery of Pyroshock Data from Distorted Acceleration Records. NASA TP 2494, 1985, pp. 1-14.

64. Moore, Donald Baker: Personal Interview. Explosive Technology, 1985.

1. REPORT NO.	2. GOVERNMENT ACCESSION NO.	3. RECIPIENT'S CATALOG NO.
NASA TP-2603		

4. TITLE AND SUBTITLE	5. REPORT DATE
Effects of Variables Upon Pyrotechnically Induced Shock Response Spectra	May 1986
	6. PERFORMING ORGANIZATION CODE
7. AUTHOR(S) James Lee Smith	8. PERFORMING ORGANIZATION REPORT #
9. PERFORMING ORGANIZATION NAME AND ADDRESS George C. Marshall Space Flight Center Marshall Space Flight Center, Alabama 35812	10. WORK UNIT NO. M-527
	11. CONTRACT OR GRANT NO.
	13. TYPE OF REPORT & PERIOD COVERED Technical Paper
12. SPONSORING AGENCY NAME AND ADDRESS National Aeronautics and Space Administration Washington, D.C. 20546	14. SPONSORING AGENCY CODE

15. SUPPLEMENTARY NOTES

Prepared by Systems Dynamics Laboratory, Science and Engineering Directorate.

16. ABSTRACT

Throughout the aerospace industry, large variations of 50 percent (6 dB) or more are continually noted for linear shaped charge (LSC) generated shock response spectra (SRS) from flight data (from the exact same location on different flights) and from plate tests (side by side measurements on the same test). A research program was developed to investigate causes of these large SRS variations. A series of ball drop calibration tests to verify calibration of accelerometers and a series of plate tests to investigate charge and assembly variables were performed. The resulting data were analyzed to determine if and to what degree manufacturing and assembly variables, distance from the shock source, data acquisition instrumentation, and shock energy propagation affect the SRS. LSC variables consisted of coreload, standoff, and apex angle. The assembly variable was the torque on the LSC holder. Other variables were distance from source of accelerometers, accelerometer mounting methods, and joint effects. Results indicated that LSC variables did not affect SRS as long as the plate was severed. Accelerometers mounted on mounting blocks showed significantly lower levels above 5000 Hz. Lap joints did not affect SRS levels. The test plate was mounted in an almost free-free state; therefore, distance from the source did not affect the SRS either. Several varieties and brands of accelerometers were used – all varieties except one demonstrated very large variations in SRS. One accelerometer gave very good repeatable results throughout the program. Instrumentation is the cause of the large variations in SRS. SRS from the same source are indeed repeatable.

17. KEY WORDS	18. DISTRIBUTION STATEMENT
Shock Response Spectra Frustum Separation Assembly Linear Shaped Charge Pyrotechnic Shock	Unclassified – Unlimited Subject Category 39

19. SECURITY CLASSIF. (of this report)	20. SECURITY CLASSIF. (of this page)	21. NO. OF PAGES	22. PRICE
Unclassified	Unclassified	59	A04

For sale by National Technical Information Service, Springfield, Virginia 22161

NASA-Langley, 1986